Progress in Oceanography xxx (2012) xxx–xxx

Contents lists available at SciVerse ScienceDirect

Progress in Oceanography

journal homepage: www.elsevier.com/locate/pocean

Nitrogen fixation in the Gulf of California and the Eastern Tropical North Pacific

Angelicque E. White [e,*], Rachel A. Foster [a,1], Claudia R. Benitez-Nelson [b], Pere Masqué [f], Elisabet Verdeny [c], Brian N. Popp [d], Karen E. Arthur [d,2], Fredrick G. Prahl [e]

[a] Ocean Sciences Department, University of California Santa Cruz, Santa Cruz, CA, USA
[b] Marine Science Program & Department of Earth & Ocean Sciences, University of South Carolina, Columbia, SC, USA
[c] Institut de Ciència i Tecnologia Ambientals, Departament de Física, Universitat Autònoma de Barcelona, Bellaterra, Spain
[d] Department of Geology and Geophysics, University of Hawaii, Honolulu, HI, USA
[e] College of Earth, Ocean and Atmospheric Sciences, 104 COAS Administration Building, Oregon State University, Corvallis, OR, USA
[f] Departament de Física & Institut de Ciència i Tecnologia Ambientals, Universitat Autònoma de Barcelona, Bellaterra, Spain

ARTICLE INFO

Article history:
Received 27 September 2011
Received in revised form 5 September 2012
Accepted 5 September 2012
Available online xxxx

ABSTRACT

Di-nitrogen (N_2) fixation plays a well-recognized role in the enhancement of primary production and arguably particle export in oligotrophic regions of the subtropical and tropical oceans. However, recent evidence suggests that N_2 fixation may also be significant in regions of the surface ocean proximate to or overlying zones of intense subsurface denitrification. In this study, we present results from a series of research cruises in the Gulf of California (GoCal) and adjacent waters of the Eastern Tropical North Pacific (ETNP). Measurements include microscopy, genomic analyses, incubations, stable isotopic measurements, and sediment traps coupled with ^{238}U:^{234}Th disequilibria. Combined, these results suggest that N_2 fixing microorganisms are present and active throughout the region, with larger sized *Richelia* and *Trichodesmium* spp. recorded within the warmer waters at the entrance to and within the GoCal, and smaller, unicellular diazotrophs observed in the cooler waters of the northern ETNP. N_2 fixation rates in the summer varied from 15–70 μmol N m^{-2} d^{-1}, with episodic blooms contributing as much as 795 μmol N m^{-2} d^{-1}. While the estimated contribution of N_2 fixation to particle export was highly variable, blooms of diatom-*Richelia* symbioses accounted for as much as ~44% of the measured summer carbon flux at 100 m. Alternately, evaluation of the N isotopic composition of sinking material and the magnitude of measured N_2 fixation rates indicate negligible to small enhancements of new production when blooms of either colonial *Trichodesmium* spp. or unicellular diazotrophs were encountered. Consistent with previous research, we also found that while fluxes of C to sediment traps are similar in winter and summer months, the efficiency of C export (export/surface productivity) in the GoCal region is elevated during summer relative to the more productive diatom-dominated winter phase of the seasonal cycle. The episodic and variable nature of N_2 fixation recorded in this region make it unlikely that new production via diazotrophic activity is solely responsible for the observed patterns of C transport efficiency; rather, we hypothesize that eolian inputs and/or efficient transport of picocyanobacterial biomass via grazing or aggregation may further explain the enhanced export efficiency observed in the GoCal summer. In sum, diazotrophy typically supports <10%, but as much as 44% of export production. The high variability of direct measurements of N_2 fixation implies that other mechanisms contribute to the seasonal invariance of C flux in this region. If this region is indicative of other oxygen minima zones with active diazotrophs, our results indicate that export-mediated feedback mechanisms between N_2 fixation and denitrification are not as strong as previously hypothesized.

1. Introduction

The inventory of nitrogen (N) in the global ocean is largely a function of microbially-mediated reduction–oxidation reactions occurring throughout the water column and in the underlying sediments. The primary metabolic processes regulating the marine N budget are di-nitrogen (N_2) fixation and denitrification/anammox (Galloway et al., 2004). N_2-fixing organisms (diazotrophs) convert a fraction of the N_2 dissolved in the surface ocean to ammonia,

* Corresponding author. Tel.: +1 541 737 6397; fax: +1 541 737 2064.
E-mail addresses: awhite@coas.oregonstate.edu (A.E. White), rfoster@mpi-bremen.de (R.A. Foster), cbnelson@geol.sc.edu (C.R. Benitez-Nelson), pere.masque@uab.cat (P. Masqué), elisabet.verdeny@uab.es (E. Verdeny), popp@hawaii.edu (B.N. Popp), karen.arthur@anu.edu.au (K.E. Arthur), fprahl@coas.oregonstate.edu (F.G. Prahl).
[1] Present address: Max-Planck-Institute for Marine Microbiology, Celsiusstr. 1, Bremen D-28359, Germany.
[2] Present address: Evolution, Ecology and Genetics Research School of Biology, Australian National University, Canberra, Australia.

0079-6611/$ - see front matter © 2012 Elsevier Ltd. All rights reserved.
http://dx.doi.org/10.1016/j.pocean.2012.09.002

which is then integrated into cellular materials used to fuel metabolism and growth, or excreted into the surrounding marine environment among other fates. In low oxygen environments, fixed N is disassembled via denitrification, a respiratory process by which certain bacteria degrade organic matter by reducing oxidized forms of N (NO_3^-, NO_2^-) to N_2. The rate-limiting controls and feedbacks driving N_2 fixation and denitrification activities ultimately set the oceanic inventory of bioavailable N and influence rates of primary productivity and particle export.

Recent reviews of global N fluxes indicate a large imbalance in the oceanic N budget that may be a consequence of either systematic underestimation of N_2 fixation or overestimation of denitrification rates (Brandes and Devol, 2002; Codispoti et al., 2001; Middelburg et al., 1996). While such an imbalance in the oceanic N budget cannot be ruled out, the relative stability of both atmospheric CO_2 concentrations (±10 ppm) and the isotopic composition of particulate nitrogen (PN) in deep sea sediments (±0.5‰) indicate a stable marine N budget over the last ~5000 years (Altabet, 2007; Deutsch et al., 2001; Gruber, 2004; Gruber and Sarmiento, 1997). Numerical models have also suggested that the total N inputs and losses in the global ocean are held in quasi-steady state by strong feedbacks between N_2 fixation and denitrification (Deutsch et al., 2007; Moore and Doney, 2007; Tyrrell, 1999). These feedback mechanisms would be tightest in regions where both denitrifying and N_2-fixing microorganisms are both present and active (Fig. 1). While the time-scales over which these competing processes influence each other are not well-defined, the mechanism is presumed to operate as follows. Local to regional upwelling of partially denitrified deep waters brings dissolved pools low in N:phosphorus (P) (relative to the Redfield benchmark of 16 N:1P) into the euphotic zone. Intrusion of these relatively N poor deep waters into the surface, if followed by stratification, are thought to favor the growth of diazotrophs once other phytoplankton consume the available reduced N. Since N_2 fixation is a source of new N, this growth should lead to enhancements of primary and export production, assuming other elements (e.g. P or iron) do not limit N uptake. Alterations in the flux of organic matter from the surface ocean can quickly lead to variability in the extent of water column suboxia, which can in turn have large positive effects on denitrification rates (Codispoti, 1989; Codispoti et al., 2001; Gruber, 2004; Kienast, 2000). In this manner, changes in subsurface denitrification rates influence nitrate limitation in nearby upwelling areas, which in turn may favor N_2 fixation, and thereby potentially alter organic matter fluxes into the denitrification zone (Fig. 1). On longer time and space scales, as these biological processes are more separated, ocean circulation rather than particle fluxes would dominate the coupling between N_2 fixation and denitrification (Codispoti, 2006; Weber and Deutsch, 2010).

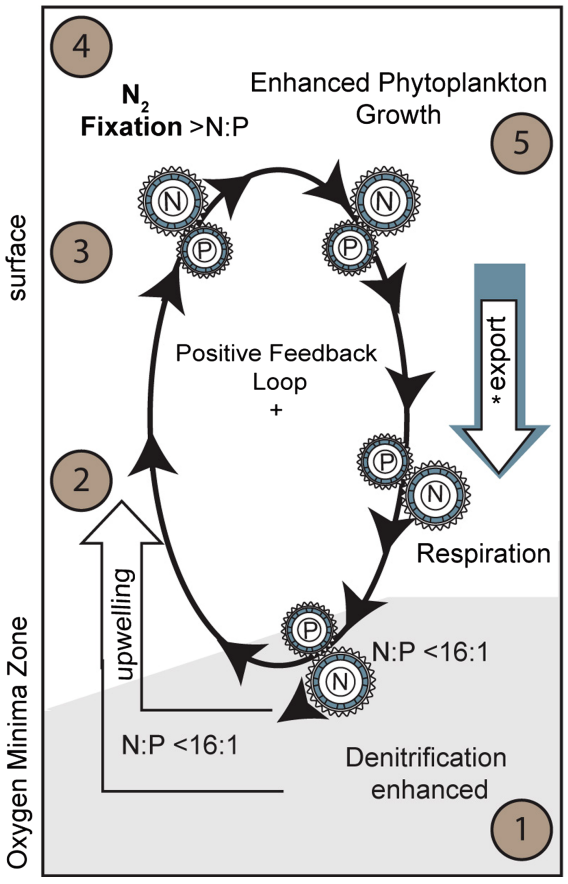

Fig. 1. Conceptual model of the potential feedbacks between primary productivity, N_2 fixation and denitrification that may occur on annual timescales. The particulate N and P of functional groups (phytoplankton, nitrogen-fixers, and denitrifying organisms) are shown as gears transforming the ratio of dissolved pools via uptake and release of elements. Upwelling of waters from the OMZ will determine the N:P ratio of nutrients available to phytoplankton in surface waters, thus controlling the magnitude of primary and export production and the maintenance of the suboxic conditions favorable for denitrification. A positive feedback loop between the processes of denitrification and nitrogen fixation would require that (1) denitrification rates are significant enough to result in N:P ratios lower than the Redfield benchmark of 16:1; (2) upwelling of denitrified waters into the euphotic zone occurs; (3) post-upwelling conditions result in warm and well-stratified surface waters; and (4) significant growth and production of diazotrophs leads to the addition of new N, P drawdown and an increase in the N:P ratio with the consequence that (5) particle export is enhanced as a result of new nitrogen inputs. Note that community composition of diazotrophic functional groups may alter export efficiency of the system.

1.1. Evidence for diazotrophy proximate to denitrification zones

A number of independent studies have provided direct biological rate measurements and/or indirect geochemical or model-based evidence to suggest that N_2 fixing organisms are present and active in each of the major oxygen minima zones associated with subsurface denitrification: during the spring intermonsoon seasons in the Arabian Sea (Bange et al., 2005; Capone et al., 1998; Dugdale et al., 1964; Prahl et al., 2000), in the Eastern South Pacific (Deutsch et al., 2007; Fernandez et al., 2011; Westberry and Siegel, 2006), and within the Eastern Tropical North Pacific (ETNP) (Brandes et al., 1998; Sigman et al., 2005; White et al., 2007a). Blooms of diazotrophs have been observed in the outer entrance zone of the Gulf of California (e.g. Mazatlan Bay, Mee et al., 1984) and high rates of N_2 fixation (White et al., 2007a) as well as episodic summer decreases in the $\delta^{15}N$ value of sinking particulate N captured in sediment traps in the central basins of the Gulf of California (e.g. Carmen and Guaymas Basin, Altabet et al., 1999; Thunell, 1998). Furthermore, analyses of paired N and O isotope measurements by Sigman et al. (2005) coupled with estimates of global and basin-scale N_2 fixation rates from the relative change of dissolved surface nitrate and phosphate concentrations (i.e., N^* or P^* values), also indicate a niche for N_2 fixation along the ETNP margin (Deutsch et al., 2007). These findings not only challenge the long held notion that marine N_2 fixation is geographically restricted to the central oceanic gyres, and therefore spatially decoupled from regions of intense subsurface denitrification (Ganeshram et al., 1995), but also indicate the potential for a more rapid feedback loop between these two opposing metabolic processes (Deutsch et al., 2007; Moore and Doney, 2007). For these reasons, oxygen minima zones are strategic study sites for evaluation of the potential feedbacks between the two dominant processes in the oceanic N budget.

Please cite this article in press as: White, A.E., et al. Nitrogen fixation in the Gulf of California and the Eastern Tropical North Pacific. Prog. Oceanogr. (2012), http://dx.doi.org/10.1016/j.pocean.2012.09.002

1.2. Regional oceanography of the Gulf of California (GoCal) and the adjacent ETNP

The ETNP is the largest region of the world's oceans characterized by subsurface suboxia. As such, it accounts for ~35–45% of global pelagic denitrification (Cline and Richards, 1972; Codispoti and Richards, 1976). The core of the ETNP oxygen (O_2) minimum zone (OMZ) is a persistent deep water mass with a >10 μM nitrate deficit (relative to Redfield stoichiometry) extending from the equator to ~25°N and westward from the coast to ~140°W (Paulmier and Ruiz-Pino, 2009). The importance of denitrification in the ETNP has been recognized for many years on the basis of (1) stoichiometric relationships between N, O_2, and P, (2) the existence of a nitrite maximum within the OMZ (Brandhorst, 1958; Cline and Richards, 1972; Thomas, 1966), and (3) observations of apparent N_2O consumption in the anoxic segment of the OMZ (Cohen and Gordon, 1978). The California Undercurrent (CU) transports these suboxic, denitrified waters from the ETNP northward into the GoCal at intermediate depths of 500–1000 m and along the continental slope of North America (Castro et al., 2001; Liu, 1992; Roden, 1958). The source water for the GoCal is then a mixture of partly denitrified subsurface waters from the south and tropical surface water flowing in from the Pacific Ocean.

Suboxia and thus denitrification are maintained by the supply of nitrate, the intensity of vertical mixing (Duteil and Oschlies, 2011), large scale circulation and ventilation rates (Gnanadesikan et al., 2012), as well as vertical and horizontal fluxes of particulate organic material supporting bacterial respiration (Van Mooy et al., 2002). Of these terms, only particle fluxes would potentially be impacted by diazotrophic production at the regional scale. Thus, the proposed coupling between diazotrophy and denitrification would require that inputs from N_2 fixation are sufficient to enhance particle export in regions overlying denitrification zones either via the sinking of diazotrophic biomass or transfer of fixed N to the remaining autotrophic community via exudation, viral lysis, or cell death and autolysis (Fig. 1). The relative contribution of N_2 fixation to particle export, however, has not been measured in a denitrification zone. In a series of cruises (Table 1: GC1, summer 2004, GC2, winter 2005; GC3, summer 2005; GC4, summer 2008) to the GoCal and adjacent waters of the ETNP, we investigated the relationship between N_2 fixation, primary productivity and particle export in order to address the broader potential for the existence of a tight regional coupling between N_2 fixation and denitrification.

2. Materials and methods

2.1. Diazotrophic community composition: epifluorescence microscopy and nifH phylotypes

In the summer of 2008, large diazotrophic organisms ($\geqslant$5 μm) were enumerated according to Carpenter et al. (2004). Briefly, bulk seawater (0.5–2.0 L) was collected via gravity flow from a rosette equipped with a conductivity-temperature-depth (CTD) system, filtered through a 5 μm pore size, 47-mm-diameter Poretics (Millipore; Billerca, MA) membrane filter and the filter mounted onto oversized (75 × 50 mm) glass slides (Corning, Harrodsburg, KY). Filaments and colonies of *Trichodesmium* as well as *Richelia,* both free-living and symbiotic with diatoms, were enumerated using an epifluorescence microscope fitted with blue (450–490 nm) and green (510–560 nm) excitation filters. Cell counts were carried out in a similar manner in 2005 (see White et al., 2007).

Nucleic acid samples (Table 2) were collected at 6–10 different depths in 2008. Seawater was collected from the CTD rosette into 2.5 L, 10% hydrochloric acid-rinsed polycarbonate bottles and 1–2 L was immediately filtered through 0.2 μm pore size Supor filters (Pall corporation; East Hills, NY) held in a 25 mm diameter Swinnex filter holder (Millipore) using a peristaltic pump. The filters were removed and placed in 1.5 mL bead beater tubes (Biospec Products; Bartlesville, OK) containing 30 μL of 0.1 mm diameter glass beads (Biospec Products), frozen in liquid nitrogen and stored at −80 °C until extracted in the laboratory for nucleic acids. Filtered DNA and RNA samples were frozen with 350 μL of RLT Buffer (Qiagen, Valencia, CA) amended with 1% β-mercaptoethanol and archived. DNA and RNA were extracted as previously described (Foster et al., 2009).

In order to identify populations actively transcribing *nifH*, total RNA was reverse-transcribed as described in Foster et al. (2009). For the qPCR assays, seven previously designed TaqMAN® (Applied Biosystems; Austin, TX) primers and probes were used to evaluate the *nifH* gene copy abundance for the following target phylotypes:

Table 1
Water column structure and nutrient composition relative to integrated N_2 fixation rates (surface to 40–60 m, approximately the 1% light level) measured within the Gulf of California (GoCal) in 2005 (GC-3, as in White et al. (2007), but presented here as N fixation rather than N_2 fixation) and 2008 (GC-4) and along the Eastern Tropical North Pacific (ETNP). All values in parentheses represent standard deviations for either the integrated rate measurement or the variability of the property within multiple casts for the station of interest.

	Date (m/yr)	N_2 Fixation (μmol N m^{-2} d^{-1})	1% Light Level (m)	Top of nitra-cline (m)	Chl max (m).	Mixed layer depth (m)	Mixed layer Temp. (°C)	Mean Si above the nitracline (μmol L^{-1})	Mean P above the nitracline (μmol L^{-1})	Mean N + N above the nitracline (μmol L^{-1})
GoCal										
Winter										
GC2	1/05	NA	30	30	14 (8.5)	20	18.8 (0.1)	12.5	1.39 (0.01)	5.50 (0.10)
Summer										
GC1	7/04	NA	24	25	26 (6)	15	28.2 (0.2)	1.9	0.51 (0.05)	0.03 (0.01)
GC3-1	7/05	43 (23)	46	40	37 (14)	10	30.4 (0.1)	3.0	0.55 (0.05)	0.08 (0.04)
GC3-2	7/05	453 (111)	35	30	38 (1)	14	29.1 (0.5)	1.6	0.65 (0.08)	0.08 (0.03)
GC3-3	7/05	61 (32)	35	30	33 (4)	7	29.9 (0.6)	3.2	0.96 (0.02)	0.04 (0.03)
GC3-4	8/05	795 (185)	48	40	46 (2)	10	29.8 (0.2)	1.8	0.66 (0.06)	0.04 (0.01)
GC4-1	7/08	20 (2)	39	30	34 (4)	15	28.2 (0.4)	1.9	0.75 (0.16)	0.09 (0.13)
GC4-2	7/08	73 (54)	48	40	46 (16)	12	29.0 (0.3)	1.4	0.49(0.05)	0.04 (0.03)
GC4-2R	7/08	56 (4)	49	30	45 (5)	10	29.6 (0.1)	1.4	0.41 (0.09)	0.04 (0.06)
ETNP										
GC4-8	7/08	14 (5)	55	70	54 (9)	11	29.3 (0.1)	1.4	0.36 (0.08)	0.08 (0.05)
GC4-9	7/08	28 (3)	48	30	40 (5)	10	28.6 (0.1)	4.4	0.64 (0.07)	0.03 (0.03)
GC4-10	7/08	127 (10)	56	30	49 (4)	15	23.4 (0.1)	2.6	0.34 (0.02)	0.05 (0.14)
GC4-11	8/08	233 (19)	50	50	50 (6)	17	20.8 (0.1)	2.8	0.31 (0.05)	0.03 (0.05)
GC4-12	8/08	29 (5)	34	25	25 (6)	22	16.8 (0.1)	0.8	0.33 (0.02)	0.22 (0.05)

Please cite this article in press as: White, A.E., et al. Nitrogen fixation in the Gulf of California and the Eastern Tropical North Pacific. Prog. Oceanogr. (2012), http://dx.doi.org/10.1016/j.pocean.2012.09.002

Trichodesmium, three symbiotic heterocystous strains (het-1, het-2, and het-3), and unicellular groups A and B (Church et al., 2005a,b; Foster et al., 2007). Unicellular group A will now be referred to as UCYN-A, the common shorthand for this group. These qPCR assays estimate the relative abundance (DNA) and mRNA expression (RNA) of known diazotrophic phylotypes. Complementary genomic analyses are invaluable for quantification of cryptic UCYN-A as well as validation of relative abundance for the other recognizable diazotrophs by microscopy.

2.2. Spatial patterns and rates of carbon and nitrogen fixation

In the summers of 2004, 2005, and 2008, *in situ* primary productivity was assessed at a series of stations in the GoCal using an *in situ* array with ^{14}C (2004, 2005; GC1, GC2 and select GC3) or ^{13}C (2005,2008; GC3 and GC4) labeled bicarbonate tracer amendments. ^{14}C and ^{13}C based rates in parallel incubations recorded in 2005 at GC3-2 were statistically equivalent with a slope of 0.83 ± 0.18 ($^{14}C/^{13}C$). Hence, we present ^{13}C surface productivity for GC3 and GC4 and ^{14}C based rates for GC1–GC2. Sampling was extended to the ETNP in 2008 (Fig. 2). The design of the free-floating array and the procedure used for its deployment followed those described by Prahl et al. (2005). All incubations were *in situ* for a period of ~24 h, from dawn to dawn. The rate of N_2 fixation was assessed on these arrays in 2005 (presented in White et al. (2007a)) and 2008 via $^{15}N_2$-uptake into particulate nitrogen (PN) (Montoya et al., 1996). Note that White et al. (2007a) present nitrogen fixation rates in units of (mol N_2 volume^{-1} time^{-1}) whereas we present them herein as (mol N volume^{-1} time^{-1}). The general procedure for preparation of these $^{15}N_2$ and ^{13}C-bicarbonate incubations is described in White et al. (2007a). Duplicate incubations were carried out at 4–5 depths between the surface and 40–60 m. A complementary set of incubations was also performed in on-deck incubators. At the end of each incubation period, suspended particles were collected by gentle vacuum filtration through 25-mm diameter, precombusted (450 °C for 12 h) glass fiber filters (GF/F). Filters were immediately stored at −20 °C in an onboard freezer. Once ashore, samples were dried overnight at 60 °C, acidified and then encapsulated in tin cups for analysis of their $\delta^{15}N_{PN}$ and $\delta^{13}C_{POC}$ (POC = particulate organic carbon) composition using the methodology described in Prahl et al. (2005). Here we assume 24-h incubations measuring the incorporation of ^{13}C-bicarbonate in particulate matter approximates net primary production (NPP) as per Marra (2002) and Halsey et al. (2010).

2.3. Particle export

In all field efforts, VERTEX-style sediment traps (Buesseler et al., 2007b) were deployed at 100 m to capture sinking material raining out of the euphotic zone. In 2008, a second set of sediment traps was also deployed at 105 m. These traps were filled with an unpoisoned NaCl brine solution and attached at the bottom of a 24 h free-floating array so that export could be coupled to *in situ* ^{13}C and ^{15}N uptake rates (see Section 2.2). Obvious swimmers were removed, following filtration of trap material for analysis of biogenic silica (bSi), particulate organic carbon (POC), PN and isotopic compositions. PC and PN and the stable isotopic composition of both were determined by high temperature combustion with mass spectrometric detection as described in Prahl et al. (2005), while bSi was measured via wet alkaline digestion as in DeMaster (1991). The isotopic composition of the PC and PN collected in these traps was used as a proxy for the contribution of N_2 fixation to export production. The ratio of ^{15}N to ^{14}N relative to that of atmospheric N_2 (expressed in delta notation as $\delta^{15}N_{PN}$) for PN produced by diazotrophs is distinctive and is characterized by $\delta^{15}N_{PN}$ values of −3‰ to 0‰ (Carpenter et al., 1997; Dore et al., 2002; Minagawa and Wada, 1986). The $\delta^{15}N$ of nitrate ($\delta^{15}N_{NO3}$) upwelled in this region was calculated by linear analysis of the ratios of the gradients of $^{14}N_{NO3}$ and $^{15}N_{NO3}$ across the nitracline (depths noted in Table 1, profiles of nitrate and nitrite in Supplementary Fig. 1) following the convention of a number of other studies (Casciotti et al., 2008; Dore et al., 2002; Popp et al., 2002) using nitrate isotope data for GC4 (J. Granger, unpublished data, analytical methods as in Sigman et al. (2001); Sulfamic acid was

Table 2
Diazotrophic community composition: *Richelia* symbioses were enumerated by the number of heterocysts per volume or via qPCR assays for het-1 and het-2 nitrogenase gene copies per volume. *Trichodesmium* concentrations were estimated as the number of filaments per volume or nifH gene copies per volume. Unicellular cyanobacteria were estimated by qPCR only.

	Dominant diazotrophic group	Abundance	Method
GoCal			
GC3-1	*Richelia* symbioses, *Trichodesmium* spp.	<100 heterocysts or filaments L^{-1}	Epifluorescence microscopy[a]
GC3-2	Richelia symbioses	300–1700 heterocysts L^{-1}	Epifluorescence microscopy[a]
GC3-3	*Richelia* symbioses, *Trichodesmium* spp.	<100 heterocysts or filaments L^{-1}	Epifluorescence microscopy[a]
GC3-4	Richelia symbioses	90–2100 heterocysts L^{-1}	Epifluorescence microscopy[a]
GC4-1	*Richelia* symbioses, *Trichodesmium* spp.	<20 heterocysts or filaments L^{-1} nifH cDNA below detection limits	Epifluorescence microscopy and qPCR
GC4-2	*Richelia* symbioses, *Trichodesmium* spp.	<40 heterocysts or filaments L^{-1}; 0–4670 het-1,2 and 0–624 *Trichodesmium* nifH cDNA copies L^{-1}	Epifluorescence microscopy and qPCR
GC4-2R	*Richelia* symbioses, *Trichodesmium* spp.	<320 heterocysts or filaments L^{-1} 0–5850 het-1,2 and 0–1110 *Trichodesmium* nifH cDNA copies L^{-1}	Epifluorescence microscopy and qPCR
ETNP			
GC4-8	*Richelia* symbioses, *Trichodesmium* spp.	<50 heterocysts or filaments L^{-1}; 20–2000 nifH cDNA copies L^{-1}[b]	Epifluorescence microscopy and qPCR
GC4-9	*Richelia* symbioses	<2 heterocysts L^{-1}, nifH below detection	Epifluorescence microscopy and qPCR
GC4-10	Group A unicellular cyanobacteria	<1000 nifH cDNA copies L^{-1}	Epifluorescence microscopy and qPCR
GC4-11	Group A unicellular cyanobacteria	<12,800 nifH cDNA copies L^{-1}	Epifluorescence microscopy and qPCR
GC4-12	Not detected	Below detection limits	Epifluorescence microscopy and qPCR

[a] At these stations, *Crocosphaera* like cells were not enumerated.
[b] Range applies to het-1, het-2 and *Trichodesmium* specific nifH gene copies.

Please cite this article in press as: White, A.E., et al. Nitrogen fixation in the Gulf of California and the Eastern Tropical North Pacific. Prog. Oceanogr. (2012), http://dx.doi.org/10.1016/j.pocean.2012.09.002

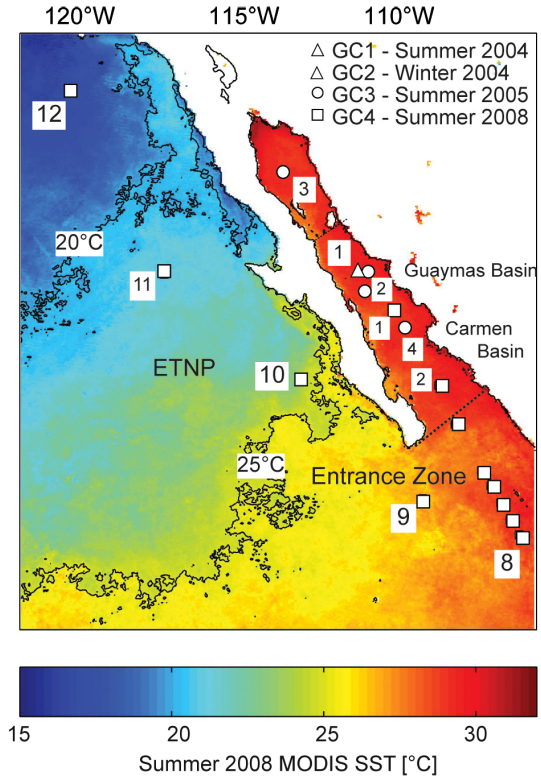

Fig. 2. Locations of sampling sites in the summer of 2004 (triangle), 2005 (circles) and 2008 (squares) overlain on the mean summer (July–September) sea surface temperature (SST) for 2008 derived from MODIS AQUA remote sensing data. Winter sampling in 2004 (GC2) was conducted at the same sampling location as GC1 The 20 °C and 25 °C isotherms are shown as solid lines for reference, with the 25 °C generally considered the boundary favorable for diazotrophy.

used to drive off nitrite (see Granger and Sigman, 2009); the coefficient of variation for $\delta^{15}N_{NO3}$ values was less than 5% with an average of 2%). The export of PN derived from phytoplankton quantitatively consuming their nitrate supply should track the isotopic composition of upwelled resources. N-depletion of the surface mixed layer (defined by nitrate + nitrite (N + N) values at or near detection limits) was pervasive at all summer sampling stations other than GC4-12 (Table 1). The fractional contribution of N_2 fixation to total measured PN export at these stations was then estimated by assuming a constant end member of 0‰ for pure N_2 fixation, the calculated $\delta^{15}N_{NO3}$ values for upwelled nitrate, and applying a simple binary mixing model (Eq. (1)) to the $\delta^{15}N_{PN}$ values of trap material (as in Dore et al. (2002) and Wada and Hattori (1976)).

$$[\%N_2 \text{ fixation} = (\delta^{15}N_{PN} - \delta^{15}N_{NO3})/(\delta^{15}N_{N2} - \delta^{15}N_{NO3})] \quad (1)$$

Given recognized problems such as "swimmer" contamination and hydrodynamic biases (e.g. Buesseler et al., 2007a) in short-term trap deployments, we paired sediment trap records with an assessment of ^{234}Th:^{238}U disequilibria in 2008 in order to better understand particle export (see compilations by Buesseler, 1998; Waples et al., 2006). Total ^{234}Th samples were collected and processed according to the MnO_2 co-precipitation technique (Benitez-Nelson et al., 2001; Buesseler et al., 2001). Briefly, 4 L seawater samples were collected at discrete depths down to 1000 m using PVC sample bottles. Samples were immediately acidified to a pH of ~2 and spiked with ^{230}Th, which acted as a yield monitor. After 8–12 h of equilibration, sample pH was increased to ~8, followed by the addition of $KMnO_4$ and $MnCl_2$ to form a MnO_2 precipitate that preferentially scavenges ^{234}Th, leaving the parent ^{238}U, in solution. After ~8 h, the precipitate was filtered onto a 25 mm quartz (QMA) filter (0.7 μm), allowed to air-dry, and counted on board using a 5 sample gas flow proportional low-level beta counter (RISØ National Laboratories, Roskilde, Denmark). Samples were recounted to obtain final background activities after six half-lives (144 days) had elapsed. After final counting, samples were chemically purified using ion-exchange chemistry and analyzed using ICPMS for ^{230}Th recovery (Pike et al., 2005). ^{234}Th fluxes were then determined at 100 m using a steady-state one-dimensional model, following the methods described in Savoye et al. (2006). Water column ^{234}Th fluxes were further compared to sediment trap derived ^{234}Th fluxes in order to obtain an estimate of sediment trap collection efficiency (Buesseler, 1991). ^{234}Th derived PC export rates were determined using the PC/^{234}Th ratio measured in particles collected with the sediment traps.

2.4. Biomass

Total PC and PN were collected at all stations to provide a measure of total microbial standing stocks (White et al., 2007a). Photosynthetic and photoprotective pigments were also quantified as a means of estimating phytoplankton biomass (chlorophyll) and functional diversity (diagnostic pigments). Briefly, particulate material was collected onto pre-combusted 25 mm GF/F by gentle vacuum filtration and stored in liquid N_2 until analysis. Samples were then cold-extracted at −15 °C in 90% acetone in polypropylene centrifuge tubes. Centrifuged extracts were analyzed by the high performance liquid chromatographic (HPLC) method of Wright et al. (1991). The relative contributions of three pigment-based size classes (pico-, nano- and micro-phytoplankton) to the total algal biomass (chl) was then estimated via the formulations of Uitz et al. (2008). The relative concentrations of diagnostic pigments for picophytoplankton (chlorophyll b and zeaxanthin), nanophytoplankton (19-hexanoyl oxyfucoxanthin or 19-Hex, 19-butanoyl oxyfucoxanthin or 19-But, alloxanthin) and microphytoplankton (fucoxanthin and peridinin) approximate contributions from picocyanobacteria, prymnesiophytes and diatoms/dinoflagellates, respectively.

2.5. Remote sensing and ocean currents

The summer (June–August) sea surface temperature (SST) field as well as daily satellite-derived chl a (chl_{sat}) for the region between 18–34°N and 106–124°W was obtained from the 4-km, level-3 MODIS AQUA data provided by NASA/Goddard Space Flight Center and accessed via http://oceancolor.gsfc.nasa.gov. Time-series (2002–2008) of chl_{sat} were extracted for select stations occupied during field campaigns to the GoCal and the ETNP. Additional 0.1° resolution SST time-series were obtained from a blended product offered by NOAA CoastWatch (http://coastwatch.noaa.gov/). This blended SST product is derived from both microwave and infrared sensors carried on multiple platforms. Mean geostrophic current velocities (assuming no motion at 2000 dbar) were derived from Argos float data for July and August climatological means (2004–2009). These data were collected and made freely available by the International Argo Project (http://www.argo.ucsd.edu) and the national programs that contribute to it.

2.6. Water column structure, nutrients and N*

Photosynthetically active radiation (PAR) was measured using a rosette mounted Biospherical PAR sensor. The position of the 1% light level at each station was calculated as the mean depth of this isolume from the CTD casts conducted nearest local noon for each station. The mixed layer depth was calculated as the depth at which potential density has increased by 0.125 kg m^{-3} of the surface value (Kara et al., 2000). Water samples for nutrient analysis

Please cite this article in press as: White, A.E., et al. Nitrogen fixation in the Gulf of California and the Eastern Tropical North Pacific. Prog. Oceanogr. (2012), http://dx.doi.org/10.1016/j.pocean.2012.09.002

were collected into pre-cleaned polyvials, and immediately frozen and stored for later analysis. Soluble reactive phosphorus (SRP, here assumed to be equal to phosphate or dissolved inorganic phosphorus, DIP) and N + N were measured by standard colorimetric methods adapted to an autoanalyzer (Strickland and Parsons, 1972). The limits of detection for these methods as applied in our lab are 0.03 μmol L^{-1} and 0.05 μmol L^{-1} for N + N and DIP respectively; coefficients of variation for replicate samples were less than 10% in both cases. The parameter coined Nstar (N^*) was calculated as in Gruber and Sarmiento (1997) by adjusting for stoichiometry of denitrification (0.87 factorial) although we do not adjust values to the global mean, i.e. using $N^* = (N\text{-}16P) \times 0.87$. Dissolved silica (Si) measurements followed the protocol of Atlas et al. (1971).

3. Results

3.1. Oceanographic conditions

In each summer expedition, we observed similar hydrographic conditions in the GoCal (Table 1): warm and shallow mixed layers (28–30 °C, ~7–15 m) with nutrient concentrations above the nitracline ranging from 1.4–3.2 μmol L^{-1} Si, 0.4–1.0 μmol L^{-1} DIP, and 0.03–0.09 μmol L^{-1} N + N. Underlying this N-poor, P-replete surface layer is a persistent deep chlorophyll maxima generally positioned just below the top of the nitracline and above the 1% light level (~30–50 m). In the adjacent ETNP, moving from the entrance zone of the GoCal north along the Baja peninsula, surface N + N, Si and DIP concentrations are similar to the GoCal region albeit with increasingly cooler waters and a deepening mixed layer (Table 1, see Fig. 2 for station locations and summer SST). In contrast, winter surface waters in the GoCal are cooler (<20 °C), N, Si, and P replete, and maintain a chlorophyll max above the nitracline (Table 1).

Examination of depth profiles of the parameter N^* obtained in summer of 2004, 2005 and 2008 (GC1, GC3 and GC4-1 through GC4-9) indicate the presence of partly denitrified subsurface waters in the GoCal (N^* of -14.8 ± 1.7 in the 100–200 m depth strata) offset by less negative N^* values in surface waters (N^* of -6.5 ± 1.7 in the upper 15 m, Fig. 3). Considering 100–200 m as the source water for upwelling in this region, the absolute magnitude of the offset of N^* values in deep waters (100–200 m) relative to surface waters (0–15 m) varies with season and along a gradient from the GoCal north into the ETNP. In our single winter sampling of the GoCal region in 2005 (GC2), the profile of N^* is monotonic with depth, and surface N^* values are not significantly different from deep values (*t*-test, $p = 0.15$, Fig. 3 and Table 3). Conversely, sampling during GC1, GC3-2 and GC3-4 in the summers of 2004 and 2005 revealed significant N^* offsets that ranged from 6.6 to 8.8 (Fig. 3, Table 3). In more extensive summer sampling in 2008 (GC4), N^* offsets ranged from 6.4 to 10.6 within the GoCal and entrance zone stations (GC4-1 through GC4-9) and was 5.8 at GC-10 to the north. There were no significant differences in surface and deep N^* values at GC4-11 and GC4-12 (Table 3).

The isotopic composition of suspended PN relative to upwelled nitrate was also used as a proxy for diagnosis of regional N_2 fixation. With the exception of GC2 (winter), GC4-8, and the adjacent ETNP stations sampled in summer (GC4-10 through GC4-12), we observed near surface suspended PN that was depleted in ^{15}N relative to samples collected below the nitracline (Fig. 4, data not available for GC3). This offset was significant for GC1, GC4-2 and GC4-9 (two-tailed heteroscedastic Student's *t*-test, $p < 0.05$) but trends towards ^{15}N depletion in suspended PN collected in near surface waters are also apparent at GC4-8 and GC4-11. Comparison of these data to surface transects of $\delta^{15}N_{PN}$ values (Fig. 5) reveal regions of low $\delta^{15}N_{PN}$ values (<9‰) within the central basins of the GoCal in 2005, the entrance zone in 2008 and at ~28°N in the ETNP off Baja. Similarly, the $\delta^{15}N_{PN}$ values of material collected in 24-h free floating sediment traps deployed in 2004, 2005 and 2008 ranged from ~8–12‰ with the lowest values at GC1 (9.0 ± 0.7‰) and GC4-11 (8.3 ± 0.1‰, Fig. 5). We have evaluated the extent to which this variability can be explained by shifts in the isotopic composition of upwelled nitrate as we transitioned from the GoCal region and north into the ETNP, out of the zone of denitrification. The $\delta^{15}N_{NO3}$ values for upwelled nitrate within the GoCal and adjacent entrance zone ranged from 10.4‰ to 14.3‰ at stations GC4-1 to GC4-10 (Fig. 5, Table 3). Values in the ETNP north of 25°N became much less positive as we moved away from the denitrification zone: upwelled $\delta^{15}N_{NO3}$ was 7.8‰ at GC4-11 and 6.3‰ at GC4-12 (Fig. 5, Table 3).

3.2. Phytoplankton community composition

In 2008, N-deficient surface waters of the GoCal (GC4-1 and GC4-2) and the entrance zone (GC4-8 and GC4-9) were dominated by picophytoplankton (Fig. 6, pico = >50% of total chl biomass as per the formulation of Uitz et al. (2008)). In contrast, at the northern most station in the ETNP (GC4-12) and below the nitracline

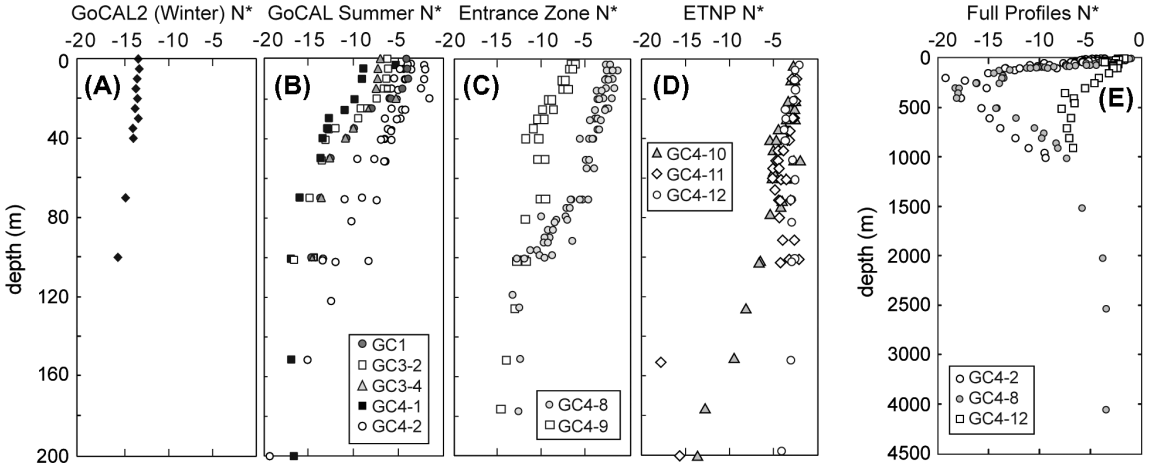

Fig. 3. N^* calculated as [(N-16P) × 0.87] for (A) winter 2005 (GC-2), (B) within the GoCal in the summer of 2004 (GC-1), summer 2005 (GC-3), and summer 2008 (GC-4) as well as (C) stations in the GoCal entrance zone and (D) north in the ETNP along the Baja peninsula. For reference, the full depth profile of N^* for GC4-2 (within the GC), GC4-8 (entrance zone) and GC4-12 (northernmost station sampled in the ETNP) are shown in (E).

Please cite this article in press as: White, A.E., et al. Nitrogen fixation in the Gulf of California and the Eastern Tropical North Pacific. Prog. Oceanogr. (2012), http://dx.doi.org/10.1016/j.pocean.2012.09.002

Table 3
The vertical offset of N*, isotopic composition of sinking material and upwelled NO_3. NA is noted when samples were not available and NS indicates stations where the potential contributions from N_2 fixation or the vertical N* offsets are not significant via a two-tailed *t*-test assuming unequal variance between samples (heteroscedastic).

	N* offset $-\left[N^*_{(100-200\ m)} - N^*_{(0-15\ m)}\right]$	100 m Sediment trap δ^{15}N-sinking PN (‰)	δ^{15}N-upwelled NO_3 (‰)	Depth range (m) for calculation of upwelled NO_3	Potential contribution from N_2 fixation via isotope mixing model
GoCal					
GC1	8.8	9.0 (0.68)	NA	NA	10–36%[a]
GC2	NS	11.7 (0.10)	NA	NA	NA
GC3-1	9.2	NA	NA	NA	NA
GC3-2	7.1	NA	NA	NA	NA
GC3-3	4.2	NA	NA	NA	NA
GC3-4	6.6	NA	NA	NA	NA
GC4-1	8.1	11.7 (0.09)	14.3	71–156	18 ± 3%
GC4-2	9.1	10.0 (0.14)	10.5	52–102	4 ± 1%
ETNP					
GC4-8	10.6	12.0	11.2	80–100	NS
GC4-9	6.4	10.8 (0.02)	NA	NA	NA
GC4-10	5.8	9.3 (1.03)	10.4	55–125	10.5 ± 9.9%
GC4-11	NS	8.3 (0.07)	7.8	60–102	NS
GC4-12	NS	9.0 (0.07)	6.3	50–100	NS

[a] Relative contributions for GC1 are calculated assuming the range of δ^{15}N values for upwelled NO_3 measured at GC4-1 and GC4-2 can be applied to GC1.

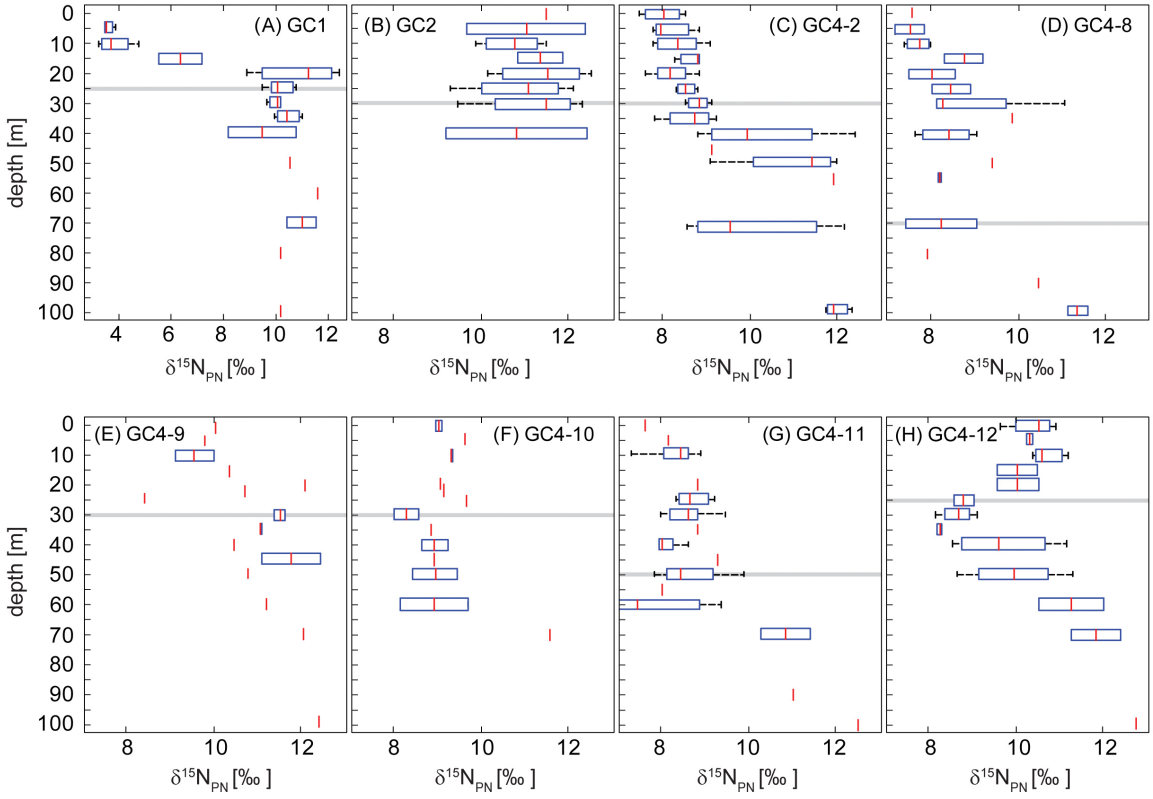

Fig. 4. Depth profiles of $\delta^{15}N$ for particulate N ($\delta^{15}N_{PN}$) at stations within the GoCal in the summer of 2004 (GC1), winter 2005 (GC2), and summer 2008 (GC4). The $\delta^{15}N_{PN}$ values for GC3 are missing due to isotopic contamination encountered during sample processing and GC4-1 are not shown as data are only available for 0–35 m. The depth of the top of the nitracline (also see Table 1) is marked as a gray line on each profile. The median for each depth is marked by a red line, box edges represent the 25th–75th percentile of the range of values, and whiskers span ±2.7 standard deviations (no box indicates only a single sample at that depth). $\delta^{15}N_{PN}$ values above the nitracline are significantly lower than values below the nitracline at GC1, GC4-2, and GC4-9 (*t*-test p values < 0.05). Note the scale change for GC1, where the largest offset of suspended $\delta^{15}N_{PN}$ values were observed. (For interpretation of the references to color in this figure legend, the reader is referred to the web version of this article.)

(>30 m) at GC4-1 in the GoCal, microscopy and pigment composition confirmed that microphytoplankton (e.g., diatoms in this case) were highly abundant. For GC4, nanophytoplankton abundances were relatively constant with depth and sampling location, ranging from ~20–45% of phytoplankton biomass (Fig. 6). These size classes roughly correspond to picocyanobacteria (*Prochlorococcus* and *Synechococcus*), cryptophytes and haptophytes (nano-), and diatoms and dinoflagellates (micro-). During GC1, GC2 and GC3 in 2004–2005, the full suite of diagnostic pigments was not analyzed by HPLC (i.e., chlorophyll b and zeaxanthin were excluded)

Please cite this article in press as: White, A.E., et al. Nitrogen fixation in the Gulf of California and the Eastern Tropical North Pacific. Prog. Oceanogr. (2012), http://dx.doi.org/10.1016/j.pocean.2012.09.002

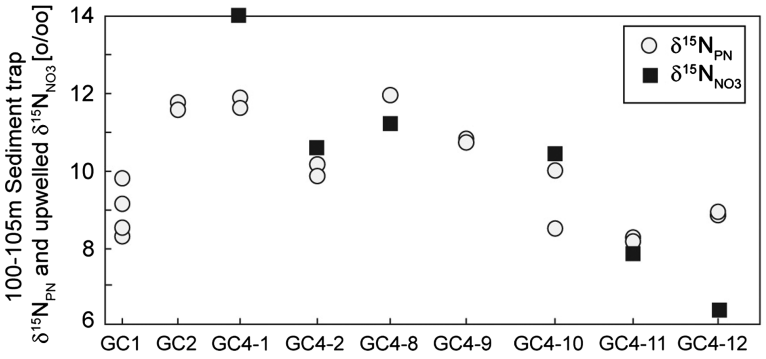

Fig. 5. The $\delta^{15}N_{PN}$ values of sinking particulate material collected over a 24-h period during cruises GC1, GC2 and GC4 in free-floating sediment traps relative to the $\delta^{15}N_{NO3}$ of upwelled nitrate. Replicate samples are shown rather than the mean with associated error bars. The $\delta^{15}N_{PN}$ values for GC3 are missing due to isotopic contamination encountered during sample processing.

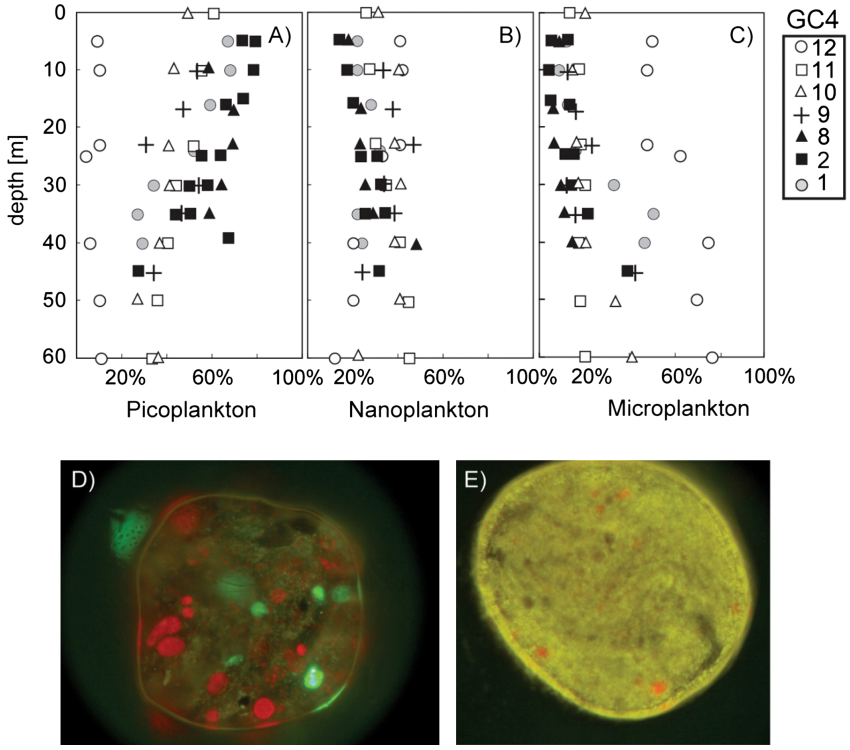

Fig. 6. Relative percentage of weighted diagnostic pigments for (A) picoplankton (chlorophyll b and zeaxanthin), (B) nanoplankton (19-Hex, 19-But, alloxanthin) and (C) microplankton (fucoxanthin and peridinin). These size classes approximate contributions from picocyanobacteria, prymnesiophytes and diatoms, respectively. Microscopic examination of sediment trap records at GC4-2 revealed picocyanobacteria (red fluorescence) in marine snow (D) and fecal pellets (E).

and so this same assessment could not be made for those study periods. However, given the persistent nutrient depletion in the GoCal in summer and the fact that GoCal assemblages are tropical in origin rather than endemic (Brinton et al., 1986), we would anticipate that picophytoplankton and other oligotrophic specialists (e.g. coccolithophores as in Malinverno et al. (2008)) dominate photosynthetic community structure in the summer phase of the seasonal cycle within the GoCal.

3.3. Nitrogen fixation rates and diazotrophic biomass

In 2008, *Richelia* (associated with *Hemiaulus* spp. hosts) were commonly observed by microscopy within the GoCal albeit in low number. At stations GC4-1 and GC4-2, depth profiles of cell abundances determined by microscopy for *Richelia* associated with the diatoms *Hemiaulus membranaceus* and *Rhizosolenia* spp. ranged from below detection to ~320 heterocysts L^{-1}. Free-living *Richelia* cells were only observed in a few samples. *Trichodesmium* spp. co-occurred with diatom symbioses, but were also in low abundance, with free filaments, including *Katagynemene* spp., more abundant (0–12 cells L^{-1}) than colonial populations (0–1 colonies L^{-1}). We observed neither the phycoerythrin containing *Crocosphaera watsonii* (3–5 μm, Group B cyanobacteria) nor the *Chaetoceros–Calothrix* symbioses in 2008.

Similar trends in abundance were revealed in 2008 using a qPCR approach (Table 2). The larger diazotrophs (*Trichodesmium* and the *Richelia* symbiotic groups het-1, het-2 and het-3) dominated within the GoCal and the entrance zone, with the highest *nifH* gene copies and gene expression recorded at GC4-2 and GC4-8. Although UCYN-A and group B were poorly detected along most of the cruise

Please cite this article in press as: White, A.E., et al. Nitrogen fixation in the Gulf of California and the Eastern Tropical North Pacific. Prog. Oceanogr. (2012), http://dx.doi.org/10.1016/j.pocean.2012.09.002

track, *nifH* gene transcription for UCYN-A was notably high at GC4-11 from the surface to 35 m (8.0×10^2 to 1.3×10^4 gene copies L^{-1}) and in a 25 m sample at GC4-10 (50 gene copies L^{-1}). The *Calothrix* symbiont that commonly associates with *Chaetoceros* diatoms was not found in any of the samples tested, nor was it observed with microscopy. Similarly, the group B unicellular phylotype was rarely detected, although our sampling was biased towards daylight hours and hence may have underestimated group B expression, which is maximized at night (Church et al., 2005a, 2005b; Shi et al., 2010). Efforts were not made to detect heterotrophic N_2-fixing proteobacteria (Zehr et al., 1998). Overall, these results indicate dominance of large diazotrophs (*Trichodesmium* and *Richelia* symbioses) within the GoCal and the entrance zone and active *nifH* transcription by small unicellular diazotrophs (UCYN-A) in the cooler surface waters of the adjacent ETNP (GC4-10 and GC4-11).

Integrated N_2 fixation rates (from surface to 40–60 m) varied throughout the study area by a factor of ~20 (Table 1, Fig. 7) with highest rates measured in the central basins of the GoCal in 2005 in accordance with a high standing stock of *Richelia* (GC3, 453–795 μmol N m^{-2} d^{-1}). In 2008 (GC4), the highest rates of N_2 fixation were recorded in the ETNP at GC4-10 and GC4-11 (Table 1). At GC4-10, integrated rates were strongly driven by a anomalous, yet replicated high rate of N_2 fixation measured at 30 m (6.9 ± 0.2 μmol N m^{-3} d^{-1}, $n = 2$). Only UCYN-A phylotypes were detected at this station with a peak abundance at 25 m (30 m was not sampled for qPCR analyses). All other depths at GC4-10 had relatively low and constant volumetric N_2 fixation rates of ~1 μmol N m^{-3} d^{-1}. Conversely, N_2 fixation rates at GC4-11 were uniformly high (6–7 μmol N m^{-3} d^{-1}) in the upper 30 m above the nitracline in water temperatures of 19–21 °C and also coincided with high abundances of *nifH* gene transcription by UCYN-A diazotrophs. Rate measurements in on-deck incubations (Fig. 8) agreed well with those from *in situ* incubations on the arrays (when data from within the mixed layer are compared, N_2 fixation on deck = 1.5 × N_2 fixation *in situ*, $r^2 = 0.99$), however elevated rates of N_2 fixation were observed in on deck incubation during the second occupation of GC4-2 and for a single incubation at GC4-8 (Fig. 8, Supplementary Table 1). With the exception of the peaks in N_2 fixation associated with blooms of varying diazotrophic phylotypes, the GoCal-ETNP region was characterized by relatively modest N_2 fixation activity (Table 1, GC4: 14–73 μmol N m^{-2} d^{-1} and GC3: 43–61 μmol N m^{-2} d^{-1}).

3.4. Relative contributions of N_2 fixation to carbon fluxes

The relative contribution of N_2 fixation to integrated primary productivity was assessed by a number of indirect methods. First, we assumed that the net C:N fixation ratio of diazotrophs approximates the 6.7 compositional benchmark for Redfield-phytoplankton. This allowed for facile conversion of N_2 fixation rates to C fixation rates for diazotrophs. This is a reasonable assumption given known elemental composition of cultured diazotrophic isolates (Krauk et al., 2006; White et al., 2006). This value was then divided by bulk ^{13}C fixation rates derived from simultaneous array incubations. In doing so, we estimate that depth-integrated N_2 fixation rates observed in the summer of 2008 accounted for less than 2% of the total C fixation at all stations, with the exception of GC4-11 where N_2 fixation accounts for 5.3% of NPP (Table 4). By comparison, N_2 fixation rates in the GoCal in 2005 accounted for 0.6–9.3% of bulk integrated C fixation, essentially two times higher than that observed in 2008. In interpreting these results, it is important to keep in mind that small contributions to primary productivity can be considerable contributions to export, as N_2 fixation is a new source of N to an N-limited mixed layer.

The relative importance of N_2 fixation to productivity and export was also assessed over longer time scales using a simple

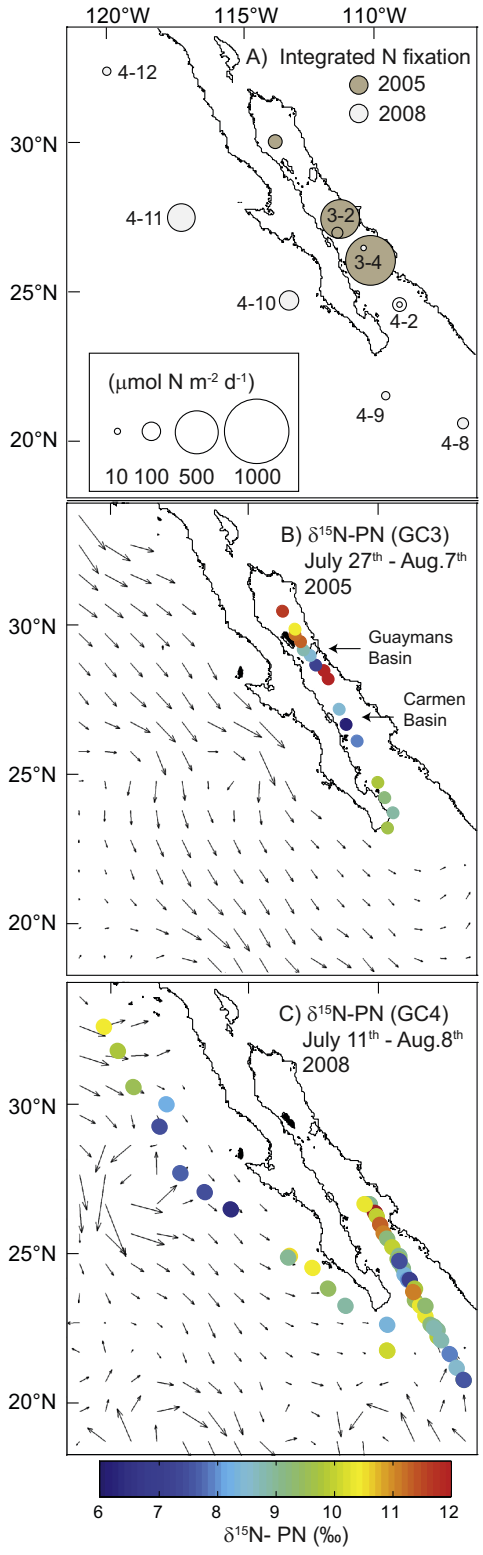

Fig. 7. (A) Nitrogen fixation rates integrated throughout the mixed layer in July–August of 2005 (brown) and 2008 (white). The area of each circle corresponds to the magnitude of the measured rate. (B and C) The isotopic composition of suspended particulate material collected in surface waters along each of these cruise tracks indicates significantly less positive $\delta^{15}N_{PN}$ values (6–8‰) relative to the $\delta^{15}N_{NO3}$ of upwelled nitrate (>10‰, Fig. 4) in (B) the Guaymas and Carmen Basins during the summer of 2005. (C) Similarly ^{15}N-depleted $\delta^{15}N_{PN}$ observed off the coast of the Baja peninsula in the ETNP (>25°N) likely reflect nitrate utilization as the upwelled $\delta^{15}N_{NO3}$ values are nearly equivalent (<8‰). In panels B–C, the mean geostrophic current velocities (assuming no motion at 2000 dbar) derived from Argos float data are also shown.

Please cite this article in press as: White, A.E., et al. Nitrogen fixation in the Gulf of California and the Eastern Tropical North Pacific. Prog. Oceanogr. (2012), http://dx.doi.org/10.1016/j.pocean.2012.09.002

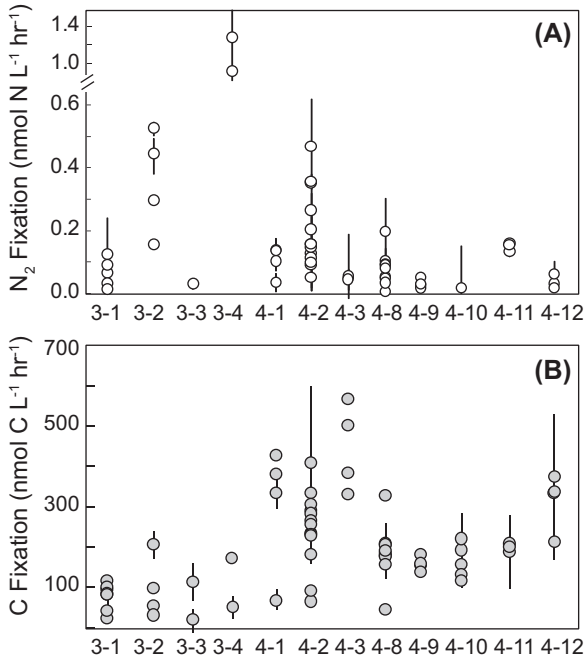

Fig. 8. (A) Nitrogen and (B) carbon fixation rates measured in on-deck incubations using water collected from within the surface mixed layer in 2005 during GC3 and 2008 during GC4. Consistent with *in situ* array data, relatively high rates of N_2 fixation were observed at GC3-2, GC3-4 and GC4-11. Contrary to arrays, rates of N_2 fixation were also found to be elevated in select incubations at GC4-2 and GC4-8. The highest volumetric rates of C fixation in these incubations were observed at GC4-1, GC4-2, GC4-3, and GC4-12. Error bars represent standard deviations.

two end-member mixing model that assumed a ^{15}N-depleted and a ^{15}N-enriched source, each representing N_2 fixation and the supply of deep nitrate, respectively. The biological input of N via diazotrophy produces particulate material with a $\delta^{15}N$ value of ~0‰ (Carpenter et al., 1997) whereas deep water nitrate in the GoCal and ETNP regions have $\delta^{15}N_{NO3}$ values of ~10–14‰ and <8‰ respectively (Fig. 5, Table 3). In applying a linear mixing model, we have assumed that N deposition (Duce et al., 2008; Krishnamurthy et al., 2007) and N recycling through zooplankton (Checkley and Miller, 1989) are insignificant complicating factors. We are not aware of any data indicating the magnitude of new N inputs via wet deposition in the region, hence we cannot fully consider this term here. In regards to N recycling, we can separate N_2 fixation and the upward diffusion of nitrate from the effects of N recycling in the euphotic zone by examining the isotopic composition of sinking PN rather than suspended PN. Since the sinking PN rain rate generally represents total N export and is in balance with new production under steady state conditions, comparison of $\delta^{15}N_{PN}$ values of sediment trap material provides a reasonable means of assessing the relative contributions of N_2 fixation and nitrate uptake to NPP (Dore et al., 2002; Wada and Hattori, 1976). Sediment trap PN material was collected for GC1, GC2, and GC4 and the $\delta^{15}N_{NO3}$ was measured in GC4. Unfortunately, isotopic results for trap materials from GC3 are unavailable. Applying a linear mixing model to GC1, GC2, and GC4 data (Eq. (1)) where the $\delta^{15}N_{N2}$ value is assumed to be 0‰ and $\delta^{15}N_{PN}$ of sinking material and $\delta^{15}N_{NO3}$ are measured, we find that the isotopic composition of particles captured in sediment traps reflect contributions of N_2 fixation on the order of 18 ± 3%, 4 ± 1% and 10.5 ± 9.5% for GC4-1, GC4-2 and GC4-10 respectively (Table 3). If we assume that the $\delta^{15}N_{NO3}$ values measured within the GoCAL during GC-4 can be applied to GC1 (~10–14 ‰), we then estimate that N_2 fixation accounts for 10–36% of the isotopic composition of sinking material in this summer occupation. At GC2 and all other GC4 stations, the $\delta^{15}N_{PN}$ value of sinking material and suspended material reflect nitrate as the exclusive source of nitrogen fueling export production (Table 3).

3.5. Surface productivity and the magnitude and efficiency of particle export

Remote sensing records (Fig. 9) for the region indicate strong accumulations of phytoplankton biomass and high seasonal estimates of primary productivity in late fall–spring months (November–April) in contrast to low standing stock and productivity in summer–early fall months (June–October, Fig. 9) when surface waters are N deficient (Fig. 10B). Indeed our direct measures of ^{13}C fixation (Table 4) follow this trend with winter C fixation generally exceeding rates determined within the GoCal in summer months. Depth-integrated ^{13}C fixation rates observed in the productive winter months of the GoCal (GC2, 91 ± 12 mmol C m^{-2} d^{-1}; Table 4, Fig. 11) were only matched at the northernmost site sam-

Table 4
Carbon fixation and PC export rates. NA indicates that data were not collected or otherwise not available. Values in parentheses represent the contribution of N_2 fixation to productivity or PC export calculated by integrated N_2 fixation * 6.67 divided by PC productivity or export. Export efficiencies are simply integrated surface productivity divided by C export.

	C fixation, mmol C m^{-2} d^{-1} and (% contribution from N_2 fixation)	Sediment Trap C export, mmol C m^{-2} d^{-1} and (% contribution from N_2 fixation)	Thorium-based C export, mmol C m^{-2} d^{-1} and (% contribution from N_2 fixation)	Trap-based C export efficiency	Th-based C export efficiency
GoCal (winter)					
GC2-1	82	12	NA	15%	NA
GC2-2	99	20	NA	20%	NA
GoCal (summer)					
GC1-1	134 ± 14	15	NA	11%	NA
GC1-2	NA	6	NA	NA	NA
GC3-1	45 ± 4 (0.6%)	19 (1.5%)	NA	42%	NA
GC3-2	43 ± 7 (7.0%)	17 (17.8%)	NA	40%	NA
GC3-3	38 ± 17 (1.1%)	12 (3.4%)	NA	32%	NA
GC3-4	57 ± 5 (9.3%)	12 (44.2%)	NA	21%	NA
GC4-1	67 ± 10 (0.2%)	18 (0.7%)	14 ± 2.7 (1.0%)	27%	21%
GC4-2	34 ± 3 (1.5%)	27 (1.8%)	19 ± 2.5 (2.6%)	79%	56%
GC4-2R	32 ± 3 (0.3%)	22 (0.4%)	30 ± 3.0 (0.3%)	69%	93%
ETNP (summer)					
GC4-8	31 ± 3 (1.2%)	28 (1.4%)	23.4 ± 0.1 (1.6%)	88%	75%
GC4-9	27 ± 5 (0.7%)	11 (1.6%)	6.6 ± 1.7 (2.8%)	43%	25%
GC4-10	47 ± 4 (1.8%)	17 (4.9%)	5.0 ± 0.7 (16.9%)	37%	11%
GC4-11	30 ± 4 (5.2%)	15 (10.7%)	18 ± 2.1(8.7%)	49%	60%
GC4-12	117 ± 8 (0.2%)	21 (0.9%)	24 ± 4.6 (0.8%)	18%	20%

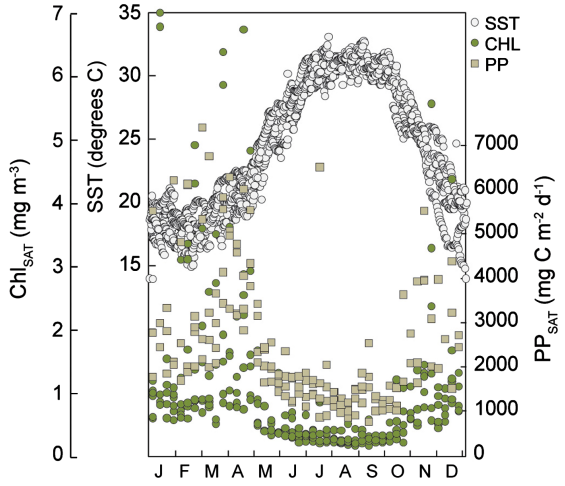

Fig. 9. The seasonal cycle of GoCal (27.5°N 117°W) sea surface temperature (SST), satellite derived chlorophyll a (Chl_{SAT}) and primary productivity (PP_{SAT}) determined from the VGPM algorithm of Behrenfeld and Falkowski (1997). The SST and Chl_{SAT} data are presented for 2002–2010 while PP_{SAT} span 2002–2007. Enhanced autotrophic biomass (as Chl_{SAT}) and primary productivity in GoCal surface waters are observed in spring (March–April) and fall–winter (October–November) months in accordance with the delivery of cold water to the surface (SST < 20 °C). Summer periods are characterized by warm (>25 °C), highly stratified surface waters with mixed layers on the order of 10–15 m (Table 1).

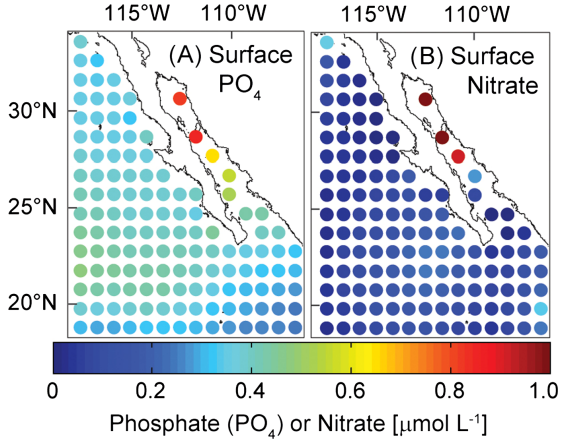

Fig. 10. Mean summer (July–September) surface phosphate and nitrate concentrations derived from World Ocean Atlas climatology. With the exception of the region north of the mid-rift islands within the GoCal, the entire region is characterized by N deficient surface waters and an excess of P.

pled in the ETNP (GC4-12, 117 ± 8 mmol C m^{-2} d^{-1}), where high microphytoplankton (diatom) standing stocks (Fig. 6) contributed to productivity, and during GC1-1 (134 ± 14 mmol C m^{-2} d^{-1}), when *Trichodesmium* colonies were observed. Otherwise, summer ^{13}C fixation rates in the GoCal region and the entrance zone ranged from 27–67 mmol C m^{-2} d^{-1}. For GC4, fluxes of bSi recorded at 100 m were highest at GC4-12 (0.91 ± 0.11 mmol bSi m^{-2} d^{-1}) and GC4-1 (0.69 ± 0.07 mmol bSi m^{-2} d^{-1}) where microscopy and pigment composition indicated a diatom-dominated community structure. At all other GC4 stations, bSi fluxes were 0.01–0.14 mmol bSi m^{-2} d^{-1}, consistent with a picocyanobacterial dominated community structure and lower integrated C fixation rates.

Particle export was assessed in ~100 m sediment traps in the summers of 2004, 2005, and 2008 and in the winter of 2005. In 2008, ^{234}Th:^{238}U disequilibria were also measured and converted to PC fluxes using the average PC/^{234}Th ratio measured in particles collected in paired 100 and 105 m sediment traps. Comparing trap and ^{234}Th-based C export (Fig. 11), we found good agreement between these independent measures of particle flux (Wilcoxon rank-sum test, $p = 0.50$; slope of linear regression = 0.97 ± 0.46, $r^2 = 0.43$). We thus compared depth integrated *in situ* ^{13}C-primary productivity (surface to 40–60 m) to sediment trap-based particle export at 100 m for all stations (GC1 through GC4) and ^{234}Th-based C export for GC4 in order to evaluate PC export efficiency. In our one winter occupation of the Guaymas Basin station of the GoCal (GC2), the rate of PC settling in 100 m traps was 15–20% of the ^{13}C-uptake based productivity in overlying surface waters (Table 4, Fig. 11). In contrast, despite the generally lower absolute C fixation rates measured in the euphotic zone in summer months, the C export efficiency recorded by sediment traps in 2005 (21–42% in GC3) was equivalent or higher than in the limited winter records (15–20% in GC2). In 2008, the efficiency of C transfer to 100 m depth was also elevated relative to our winter occupation. At stations GC4-2, GC4-2b (sampled only 6d after our first occupation, GC4-2), GC4-8 and GC4-11, sediment trap records and ^{234}Th-based PC flux estimates indicate absolute rates of C export ⩾50% of integrated ^{13}C-based primary productivity (Fig. 11C).

We estimated the contribution of N_2 fixation to PC flux by converting N_2 fixation rates to diazotrophic C fixation using the 6.7 Redfield C:N molar ratio (Redfield, 1958), and dividing these estimates by measured sediment trap (GC1 through GC4) and ^{234}Th-based (GC4) PC flux rates (Table 4). This approach views N_2 fixation as de facto new production (Eppley and Peterson, 1979). For GC3, diazotrophic C fixation is equivalent to 1.5–3.4% of the PC flux recorded by sediment traps at those stations with low N_2 fixation (GC3-1, GC3-3) and 18–44% of the PC flux at GC3-2 and GC3-4 where blooms of *Richelia* symbioses were observed (White et al., 2007a). For GC4 stations GC4-1, GC4-2, GC4-2b, GC4-8, GC4-9, and GC4-12, where N_2 fixation rates were less than 100 μmol m^{-2} d^{-1}, estimated diazotrophic C fixation is equivalent to 0.3–2.8% of C flux derived by either ^{234}Th or sediment trap based PC flux estimates. Lastly, at GC4-10 and GC4-11, where UCYN-A populations were detected, the estimates of diazotrophic C fixation were equivalent to 4.9 ± 0.4% (GC4-10) and 10.7 ± 0.9% (GC4-11) of sediment trap PC flux rate and 16.9 ± 1.3% (GC4-10) and 8.7 ± 0.7% (GC4-11) of ^{234}Th-based PC flux. When both sediment trap and isotope data are available (e.g. GC4), the relative contribution of diazotrophs to export estimated from rate measurements (0.3–17% for GC4) agrees well with the results from a linear mixing model applied to the $\delta^{15}N_{PN}$ values sediment trap material (4–18% for GC4, Table 3). While these calculations illustrate the difficulty in comparing processes occurring on disparate temporal and spatial scales (N_2 fixation and particle export), it is also clear that the magnitude of N_2 fixation observed in this region can episodically account for a sizeable fraction (up to ~40%) of the measured sinking PC flux in summer.

4. Discussion

This research was initiated to test the hypothesis that N_2 fixation appreciably contributes to particle flux in a region overlying a prominent zone of denitrification. We have employed a number of tools to assess the biological imprint of N_2 fixation in this region, including determination of the isotopic composition of suspended and sinking particulate material, direct measures of N_2 fixation rates and diazotrophic biomass, evaluation of trends in nutrient stoichiometry (N*), and two independent measures of particle flux. While the composite results are nuanced, our work has resulted in four major findings:

1. In summer the entrance zone and the basins of the GoCal alternately support large cell-sized diazotrophs of the genus *Richelia* or *Trichodesmium* whereas the cooler surface waters of the ETNP support small group A unicellular diazotrophs.

Please cite this article in press as: White, A.E., et al. Nitrogen fixation in the Gulf of California and the Eastern Tropical North Pacific. Prog. Oceanogr. (2012), http://dx.doi.org/10.1016/j.pocean.2012.09.002

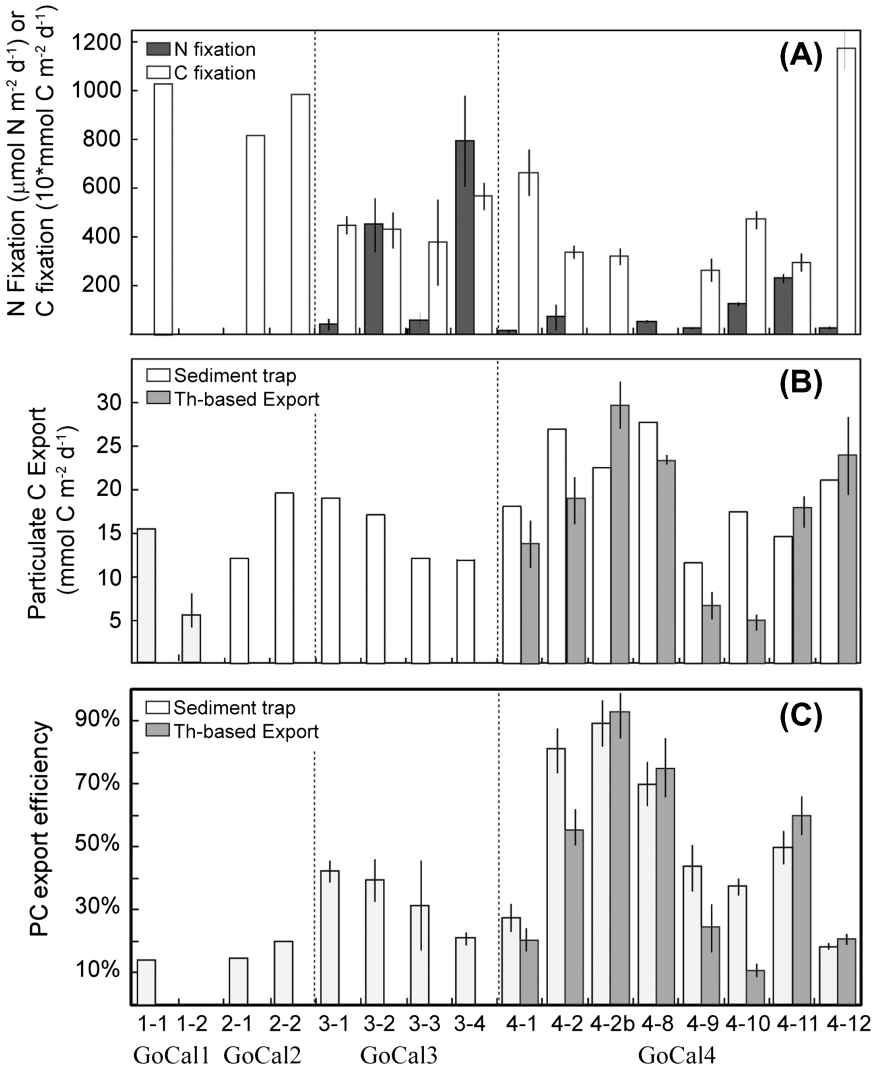

Fig. 11. (A) Water-column (~0–60 m) integrated N and C fixation for GC2 (winter 2004), GC3 (summer 2005 with *Richelia* blooms at GC3-2, GC3-4) and GC4 (summer 2008 with a bloom of UCYN-A at GC4-11) relative to (B) the particulate C export measured in sediment traps and via ^{234}Th:^{238}U disequilibria calculated using the sediment trap C:^{234}Th ratio (see text for details). (C) The PC export efficiency calculated as the percentage of C recovered in traps or via ^{234}Th scavenging divided by the integrated water column C fixation for that station. Dashed lines separate sampling years.

2. The GoCal and adjacent ETNP region is characterized by a modest background level of integrated N_2 fixation in summer (15–70 μmol N m^{-2} d^{-1}) with blooms of undetermined frequency that lead to significant enhancements of areal N_2 fixation rates (453–795 μmol N m^{-2} d^{-1}).
3. Independent calculations based on both direct N_2 fixation rates relative to particle export and the isotopic composition of settling material relative to upwelled nitrate indicate that diazotrophy typically supports <10%, but episodically as much as 44% of PC export at 100 m.
4. The rate and efficiency of PC export in the summer equals or exceeds that observed in limited winter sampling. The relatively high values of export efficiency observed in summer are not well matched with interannual and spatial trends in integrated N_2 fixation rates suggesting that in addition to N_2 fixation, other mechanisms operate to explain the seasonal invariance of PC flux in this region. Here we propose that small cell size dominated communities lead to enhanced efficiency of PC export in summer months in the GoCal when these organisms dominate phytoplankton community structure.

We will first discuss each of these major points and then turn to a consideration of what these composite findings tell us about the potential regional coupling of N_2 fixation and denitrification. Beginning with the habitat itself: the surface waters of late summer in the GoCal and throughout the adjacent ETNP region have low to undetectable quantities of fixed nitrogen, with ~0.5–1.0 μmol L^{-1} of residual DIP (Fig. 10), which from a macronutrient perspective suggests the region would be uniformly well-poised to support N_2 fixation-based new production. In addition to these seemingly stable surface nutrient conditions, we find diazotrophic phylotypes partitioned into clear niches based on temperature. Specifically, warm summer waters of the GoCal and the entrance zone support large-cell sized diazotrophs while the cooler ETNP harbors small unicellular diazotrophs. *Trichodesmium* (~7 μm in cell length and often strongly buoyant due to gas vesicles) and *Richelia* species (symbionts of diatom hosts having cell lengths >50 μm and capable of high sinking fluxes) are generally believed to be confined to calm, well-stratified, and warm (typically ⩾~25 °C) surface waters (Capone et al., 1997; Foster and O'Mullen, 2008; White et al., 2007b). Hence, it is not entirely

Please cite this article in press as: White, A.E., et al. Nitrogen fixation in the Gulf of California and the Eastern Tropical North Pacific. Prog. Oceanogr. (2012), http://dx.doi.org/10.1016/j.pocean.2012.09.002

surprising to find these organisms intermittently thriving in the GoCal. We have not, however, observed both types of large diazotrophic blooms at any one occupation. In the summer of 2004 (GC1), the isotopic composition of surface suspended particulate material [low $\delta^{15}N_{PN}$ values (3.5‰) and high $\delta^{13}C_{PC}$ values (~−15‰) (see White et al., 2007a)] and the abundance and composition of the alkane *n*C17, known to be dominant in *Trichodesmium* [$\delta^{13}C$ of *n*C17 = −13‰ (White et al., 2007a)], indicated *Trichodesmium* spp. activity that was absent in later sampling in 2005 and 2008. Alternately, in the summer of 2005 (GC3, Table 2), large surface blooms of *Richelia*-diatom symbioses were observed in the central basins of the GoCal (White et al., 2007a). Finally, in summer 2008 we encountered lower diazotrophic biomass and lower productivity at all stations in the summer of 2008. There was one unexpected exception at the N-deficient, 19–21 °C waters of GC4-10 and GC4-11 in the ETNP, where high concentrations of Group A diazotrophs (UCYN-A) coincided with a region of low $\delta^{15}N$ values (<8‰) in surface suspended material (Table 2, Fig. 7). This latter finding is in line with a growing body of work indicating that UCYN-A have broader latitudinal distributions, occur deeper in the water column, within upwelling zones (Fernandez et al., 2011; Foster et al., 2009), and at colder temperatures and higher latitudes than large cell-sized diazotrophs (Moisander et al., 2010; Needoba et al., 2007). Thus, within the larger functional group of diazotrophs, we find apparent temporal and spatial partitioning of oceanic niches within the GoCal-ETNP habitat. Diversity notwithstanding, we now have three summer records of diazotrophs present and active in surface waters atop a denitrification zone.

Mirroring the observed variability in diazotrophic phylogeny and standing stocks, direct measurements of $^{15}N_2$ fixation varied widely between stations/depths along a single cruise transect and between successive sampling years. Overall, summers in the GoCal region are characterized by a background N_2 fixation rate of 15–70 μmol N m^{-2} d^{-1} overlain by episodic blooms (453–795 μmol N m^{-2} d^{-1}). It is important to note here that what we have called 'background' levels are similar to mean estimates of N_2 fixation measured in other regions of the Pacific. Specifically, Church et al. (2009) estimate the mean N_2 fixation rate for the oligotrophic North Pacific subtropical gyre to be 111 ± 66 μmol m^{-2} d^{-1} and a recent synthesis of global diazotrophic rates by Luo et al. (2012) indicates that the geometric mean for the North Pacific Ocean (0–55°N) is between 67 and 90 μmol m^{-2} d^{-1}. The blooms that we have observed are extraordinary in magnitude for the broader Pacific, while 'background' rates are not dissimilar from the range of other measurements reported for the basin.

The next relevant test of the coupling hypothesis (Fig. 1) is whether or not the abundance and activity of diazotrophs impacts NPP and particle export. We have assessed the potential contribution of diazotrophs to primary productivity at multiple scales by (1) conversion of daily N_2 fixation rates to estimated diazotrophic C fixation, and (2) using N^* profiles as potential indices of P consumption in the absence of fixed N – a hallmark of diazotrophy. The daily contribution of N_2 fixation to integrated C fixation was estimated by conservatively assuming that net C:N fixation rates for diazotrophs can be approximated by the Redfield ratio. As a result we find that diazotroph activity is equivalent to 0.2–9.2% of integrated C fixation during GC3–GC4. These estimates represent an absolute lower bound for the diazotrophic contribution to C fixation given that the mean C:N fixation ratios measured in isolated natural populations of *Trichodesmium* spp., and diatom-*Richelia* symbioses span from 13–198 mol C fixed per mol N fixed (Mulholland, 2007) and $^{15}N_2$ tracer assays are now thought to significantly underestimate *in situ* N_2 fixation (Mohr et al., 2010). In order to scale up from daily integrated productivity rates, we also attempted to diagnose spatial patterns of N_2 fixation by examining vertical offsets in N^* (Fig. 3, Table 3). This analysis assumes that the process of N_2 fixation would consume P without a concomitant drawdown of N and thus lead to less negative surface N^* values and a larger N^* offset. Significant N^* offsets (4.2–10.6) were observed for GC1, GC3, and GC4, extending from GC4-1 to GC4-10, where UCYN-A were detected (Table 2). N^* values at depth were not significantly different than surface N^* for GC4-11 and GC4-12 (Table 3). This trend is consistent with a significant P drawdown in N deplete surface waters of the GoCal and entrance zones that can potentially be attributed to the integrated impact of N_2 fixation. The variability in the magnitude of these N^* offsets, i.e. the degree of P drawdown could also be due to (1) shifts in P resource utilization, caused by plasticity in cell physiology or shifts in phytoplankton community composition (as in Geider and Roche, 2002), and/or (2) changes in the advective link between upwelled nutrient inputs and the strength of denitrification at depth. Given that the N^* offsets we calculate are relative to the actual deep N^* values, changes in deep-water circulation or mixing of water masses (Weber and Deutsch, 2010) should not influence our interpretation. Nonetheless, given the potentially confounding factors driving the magnitude of N^*, we cannot interpret these offsets as reflecting solely the balance of denitrification and N_2 fixation. Conservatively however, these trends are consistent with temporally integrated N_2 fixation within the GoCal and at stations as far north as GC4-10 during summer.

Up to this point, we have documented N_2 fixation rates in the euphotic zone, which vary by nearly two orders of magnitude. With caveats, N^* offsets suggest the variability in rates may be smoothed over time and by prevailing circulation, such that the surface mixed layer at all summer GoCal stations indicates significant P drawdown in the absence of fixed N. Under a steady state assumption, these diazotrophic N inputs must be exported otherwise N would build up in the mixed layer. Indeed N_2 fixation in the GoCal does appear to intermittently support a significant fraction of PC export, specifically during blooms of diatom-*Richelia* symbioses (GC3).

By converting N_2 fixation rates into C fixation rates assuming a Redfield ratio for C/N (6.7), we calculated that the input of new N via diazotrophy accounts for as much as 44% of PC fluxes at 100 m when *Rhizosolenia–Richelia* blooms were present (Table 4). In other summers (GC1 and GC4), the conversion of N_2 fixation to new C-based production as well as independent assessments of the isotopic composition of PN in sinking material relative to the $\delta^{15}N_{NO3}$ values of upwelled nitrate (Table 3), suggest that N_2 fixation accounts for 0–18% of PC export when either the buoyant colony forming *Trichodesmium* or small unicellular diazotrophs (UCYN-A) appear to dominate the diazotrophic community structure. The absolute magnitude of these contributions come with a measure of uncertainty as PC flux determined from sediment traps and ^{234}Th disequilibrium, daily N_2 fixation rates, and diazotrophic contributions estimated via the isotopic composition of sinking PN each represent different temporal (days-weeks) and spatial scales of observation. What we can say with certainty is that independent metrics indicate measurable contributions of N_2 fixation to short-term particle export, i.e. N_2 fixation can be a significant albeit intermittent N input term in this region. In fact, the notion that diazotrophy can lead to increased particle flux is not new. N_2 fixation has been suggested to enhance export fluxes of C and N in the North Pacific subtropical gyre (Dore et al., 2002; Scharek et al., 1999) and in the Baltic Sea (Struck et al., 2004), among other sites. This enhancement may be a consequence of direct settling of organic material in the case of blooms of the symbiont *Richelia*, packaged inside the relatively heavy silica shells of their host diatom (e.g. Armstrong et al., 2001). In the case of strongly buoyant *Trichodesmium* or small, unicellular diazotrophs, diazotrophic contributions to particle flux can occur via grazing pathways or supply of

Please cite this article in press as: White, A.E., et al. Nitrogen fixation in the Gulf of California and the Eastern Tropical North Pacific. Prog. Oceanogr. (2012), http://dx.doi.org/10.1016/j.pocean.2012.09.002

new N to other phytoplankton followed by aggregation and incorporation of N into settling detritus, rapid grazing or reduced remineralization. Without delineating the exact pathways, the net result of our multi-year research effort supports the hypothesis that N_2 fixation in the GoCal and ETNP, primarily under bloom scenarios, can contribute significantly to particle export.

Our field work has revealed that the two-layered structure of the euphotic zone in the GoCal (as in Coale and Bruland (1987) and Small et al. (1987)) consists of an upper layer which is N-deficient and poised for N_2 fixation and the lower layer lying atop a steep nitracline that governs more classical types of primary production (e.g. nitrate-driven). N_2 fixation appears to provide one mechanism to enhance particle export from the N-deficient upper layer, however this process appears to be episodic and the estimated magnitude of diazotrophic contributions to export are variable (Table 4). Satellite-based records of phytoplankton biomass (Chl_{SAT}) and proxies of primary production (PP_{SAT}) within the Guaymas Basin of the GoCal where N_2 fixation has been recorded, indicates that Chl_{SAT} and PP_{SAT} are higher in winter than in summer (Fig. 9A). Yet, vertical fluxes of PC and PN show no such corresponding seasonality. In fact, PC flux measured at 500 m with sediment traps is uniformly ~1–2 mmol C m^{-2} d^{-1} throughout the year (Altabet et al., 1999; Thunell, 1998). These disparate surface and deep water trends imply that the efficiency of 'export' production in summer must be greater than that in winter. Indeed our research support this earlier work: relative to limited winter sampling, summer occupations in the GoCal and adjacent ETNP revealed an upper water column largely dominated by picocyanobacteria, modest N_2 fixation and highly efficient transport of PC to depth as estimated by ratios of C fixation to PC export. Additionally, since diatoms were only abundant in the most northern station of our ETNP sampling region (GC4-12), large, rapidly sinking phytoplankton (e.g. diatoms) do not appear to be requisite for efficient PC export in this region. In fact, when pigment analyses and microscopy indicated a diatom-dominated phytoplankton community structure, PC export efficiencies were moderate (PC export/C production = 18–20% at GC4-12). Only during GC1, when the buoyant diazotroph *Trichodesmium* was presumably active and abundant, was PC export efficiency estimated to be lower (11%, Table 4). The highest export efficiencies (PC export at or exceeding 50% of integrated primary productivity, Fig. 11, Table 4) were at stations dominated by picocyanobacteria (e.g. GC4-2, GC4-8). The absolute magnitude of these efficiency estimates may be artificially high due to lateral inputs of material that would lead to uncoupling of new and export production or temporal offsets that we cannot account for: e.g., bloom events prior to sampling. Nonetheless, the repeated (2005, 2008) observations of high C transfer efficiencies in the GoCal region in summer despite widely varying rates of N_2 fixation suggest that diazotrophy alone is not a sufficient explanation for the observation that PC fluxes in this region appear uncoupled from seasonal trends in surface productivity as perceived from ocean color.

To then address the question of what is leading to these high efficiency terms, visual examination of trap materials showed no evidence of empty diatom frustules, but rather we observed picocyanobacteria encased in marine snow and packaged in fecal pellets (Fig. 6D and E). An unexpected outcome of this work, then relates to the question: How would small-cell dominated water columns lead to efficient vertical transport? Richardson and Jackson (2007) report that picocyanobacteria can effectively contribute to particle export via aggregation into marine snow and/or mesozooplankton grazing at rates proportionate to gross productivity. Aggregation may also be related to seasonality of nonbiogenic, inorganic eolian or fluvial inputs to surface waters. Nearly 70% of annual precipitation in the GoCal region occurs in summer months, (Baumgartner et al., 1991), which are also characterized by the highest seasonal fluxes of terrigenous material (Lyons et al., 2011; Thunell, 1998). These inputs may bring potentially limiting trace elements that could fuel growth (e.g., iron), but may also promote aggregation and provide the ballast needed for small picocyanobacterial cells to settle (Thunell, 1998). Seasonal shifts in the elemental composition of sinking organic material may also help to explain increased PC export efficiency in the summer phase of the GoCal region. Lyons et al. (2011) report that POC:POP ratios of material reaching sediment traps moored at 500 m in Guaymas Basin are significantly higher in summer than winter, suggesting either preferential remineralization of POP in summer and/or enhanced POC content of sinking material. Whether it be via alteration of elemental stoichiometry, Fe-fueled growth and export, inputs of eolian POC and aggregation of small cells, clearly there are viable mechanisms for efficient particle export in the warm, stratified summers of the GoCal that may not depend on N_2 fixation. Moreover, our finding that the efficiency of C transport can be elevated when small cells dominate the upper water column is in line with a growing, but underappreciated, body of literature (Lomas and Moran, 2011; Richardson and Jackson, 2007; Turley and Mackie, 1995).

5. Summary and conclusions

The global ocean N budget is largely balanced by the opposing processes of denitrification and nitrogen fixation. These competing metabolic modes set the inventory of fixed N in the ocean which ultimately acts to control biological productivity and C sequestration in the sea. Since the seminal papers of Gruber and Sarmiento (1997) and Codispoti et al. (2001), researchers have examined estimates for the magnitude of denitrification and N_2 fixation in an attempt to diagnose shifts in past and present oceanic C and N budgets (Altabet, 2007; Deutsch et al., 2007; Deutsch and Weber, 2012; Galloway et al., 2004; Ganeshram et al., 1995; Gruber, 2004). In his compendium, Gruber (2004) discussed several potential stabilizing and destabilizing feedbacks governed by the differential impact of N_2 fixation and denitrification on surface productivity, N:P ratios, oxygen levels, and export production. These internal versus external controls of the global N budget may explain the seemingly paradoxical conclusion that is derived from interpretations of global N:P ratios; that the marine N budget is approximately in balance, while direct rate measurements (if accurate) imply a N deficit. Feedback mechanisms could operate on the time scale of ocean turnover, i.e. centuries, and lead to Gruber's (2004) 'nitrogen cycle homeostat' that allows for high frequency transient imbalances in context of a longer term steady state condition.

Inherent in these earlier works was the implicit assumption that a strong spatial separation existed between N_2 fixation and denitrification (Deutsch et al., 2004; Gruber, 2004). The work we have presented here is in a way a test of this last assumption. We have found that in fact N_2-fixing organisms are present and active in relatively close spatial proximity to a region of active denitrification, i.e. the processes of nitrogen fixation and denitrification are not spatially disconnected. Recent findings in other OMZ's support our finding. Fernandez et al. (2011) report nitrogen fixation rates of 48 ± 68 μmol N m^{-2} d^{-1} in the euphotic zone of the coastal upwelling zone of the Eastern Tropical South Pacific and 574 ± 294 μmol N m^{-2} d^{-1} in the underlying oxygen-deficient waters. Hamersley et al. (2011) measured areal N_2 fixation rates of ~150 μmol N m^{-2} d^{-1} in the hypoxic basins of the Southern California Bight, in accordance with detection of UCYN-A in the photic zone and heterotrophic *Alpha* and *Gammaproteobacteria* in deep hypoxic waters. Finally, Jayakumar et al. (2012) measured gene expression of *Trichodesmium* and proteobacterial nifH phylotypes in the oxygen deficient zone of the Arabian Sea.

Please cite this article in press as: White, A.E., et al. Nitrogen fixation in the Gulf of California and the Eastern Tropical North Pacific. Prog. Oceanogr. (2012), http://dx.doi.org/10.1016/j.pocean.2012.09.002

With this new understanding, an emerging theoretical framework (Deutsch et al., 2007; Moore and Doney, 2007) suggests that close geographical proximity of these processes results in tighter coupling between source and sink terms, preventing large swings in the oceanic N inventory. As we have outlined in the introduction, this coupling requires that diazotrophy proceeds at rates sufficient to impact particle export. The model of Deutsch et al. (2007) for example predicts that N_2 fixation could support upwards of 50% of particle export in OMZ regions. While we can confirm that the activity of diazotrophs can result in significant contributions to new and export production (up to 44% of export), the majority of our observations reflect a much more modest signal (a median contribution to export of 1.7% when based on measured N_2 fixation rates versus a median of 5% when based on isotope mixing models, Tables 3 and 4). Unless we have undersampled blooms of N_2 fixers, the high variability of observed N_2 fixation rates as well as the low median contributions to export indicated by direct rates and isotope mixing models are inconsistent with N_2 fixation as a persistent contributing source to export production. For comparison, Casciotti et al. (2008) used the same isotope mixing model approach applied herein and calculated that N_2 fixation supplied between 0 and 44% (average = 24 ± 19%) of exported N in the summer of 2004 at Station ALOHA in the North Pacific subtropical gyre – a region where N_2 fixation is assumed to play a large role in biogeochemical dynamics (Karl and Letelier, 2008). There is then little direct evidence to support persistent contributions of N_2 fixation to particle export in excess of 50% as predicted by the model of Deutsch et al. (2007).

This brings us to the crux of the regional N_2 fixation–denitrification coupling hypothesis (Fig. 1). When integrated over time (as in models), can pulsed inputs of new nitrogen via N_2 fixation lead to persistent summer enhancement of export? Would median contributions to summer particle export of <10% impact the maintenance of bottom water hypoxia? While we cannot quantitatively answer these questions without either integrative metrics of N_2 fixation and/or estimates of bacterial carbon demand and water column respiration of sinking material, the apparent stochasticity of diazotrophy indicates to us that the feedbacks between regional scale N_2 fixation and denitrification are not as strong as previously hypothesized, at least not in the ETNP and GoCal. Rather, the pattern and magnitude of measured rates suggests the potential for frequent and transient imbalances (as in the 'nitrogen cycle homeostat' of Gruber (2004)) which would be smoothed to a longer term mean N balance by large scale circulation on the time scales of ocean turnover (also see Deutsch and Weber, 2012). Hence, while waters with a recent history of denitrification may help stimulate N_2 fixation, it is not clear that N_2 fixation regularly or directly impacts denitrification in turn. Unless large blooms are a more frequent occurrence than our limited sampling suggests, it would appear that the coupling hypothesis presented operates on longer time-scales than could be sampled via a traditional oceanographic field campaign.

Finally, there are clearly other mechanisms that modulate the efficiency of vertical PC export in this system. We have hypothesized that a combination of allochthonous inputs followed by aggregation and sinking of small cells and/or highly efficient mesozooplankton grazing of picocyanobacteria may explain the large carbon export signal observed in summer relative to seasonally depressed primary productivity in surface waters. This hypothesis could be tested by continued study using sediment trap time-series and or novel experimental approaches such as biomarker and/or molecular biological tracers. Other potential means of enhancing export efficiency in this system include preferential remineralization of N and P from sinking organic matter and/or excess C uptake by phytoplankton (Deutsch and Weber, 2012).

In conclusion, while we cannot rule out local feedbacks between N_2 fixation and denitrification, over our relatively short observational record (4 yr), N_2 fixation only transiently leads to greater than 10% enhancements of PC export. We hypothesize that other mechanisms (e.g. picocyanobacterial aggregation) are more likely explanations for the observations of enhanced PC export efficiency in summer. Perhaps the ongoing revisions of the classic $^{15}N_2$ fixation assay will bring rate based estimates of global N_2 fixation closer in line with large scale spatial and temporal patterns diagnosed by geochemical proxies and the time-scale of the coupling hypothesis can be revisited.

Acknowledgements

Support for this project was provided by NSF OCE-0726422 (FP), NSF OCE-0726543(BNP), NSF OCE-0726290 (CBN), NSF OCF-0962362 (AW), MEC CTM2007-31241-E/MAR (PM), EU FP7-MC-IIF-220485 (CBN and PM) and the ICREA Academia, funded by the Generalitat de Catalunya (PM). Sample processing by RAF was supplemented with funds provided by the Center for Microbial Oceanography: Research and Education (C-MORE) and the Gordon and Betty Moore Foundation. FP is grateful to the Science and Technology Center for Coastal Marine Observation and Prediction for partial support in this research endeavor, through cooperative agreement in the National Science Foundation Division of Ocean Sciences (OCE-0424602). This is SOEST contribution number 8758. We thank Natalie Wallsgrove, Renee Styles, and Viena Puigcorbé for sample collection and analyses. Julie Granger provided generous and helpful comments on an early draft and kindly provided nitrate isotope data.

Appendix A. Supplementary material

Supplementary data associated with this article can be found, in the online version, at http://dx.doi.org/10.1016/j.pocean.2012.09.002.

References

Altabet, M., 2007. Constraints on oceanic N balance/imbalance from sedimentary ^{15}N records. Biogeosciences Discussions 4, 75–86.

Altabet, M.A., Pilskaln, C., Thunell, R., Pride, C., Sigman, D., Chavez, F., Francois, R., 1999. The nitrogen isotopes biogeochemistry of sinking particles from the margin of the Eastern North Pacific. Deep-Sea Research I 46, 655–679.

Armstrong, R., Lee, C., Hedges, J., Honjo, S., Wakeham, S., 2001. A new, mechanistic model for organic carbon fluxes in the ocean based on the quantitative association of POC with ballast minerals. Deep Sea Research Part II: Topical Studies in Oceanography 49, 219–236.

Atlas, E.L., Hager, S.W., Gordon, L.I., Park, P.K., 1971. A Practical Manual for Use of the Technicon Autoanalyzer in Seawater Nutrient Analyses; Revised. Technical Report. Oregon State University, p. 48.

Bange, H., Naqvi, S., Codispoti, L., 2005. The nitrogen cycle in the Arabian Sea. Progress in Oceanography 65, 145–158.

Baumgartner, T.R., Ferreira-Bartrina, V., Moreno-Hentz, P., 1991. Varve formation in the central Gulf of California: a reconsideration of the origin of the dark laminae from the 20th Century varve record. In: Dauphin, J.P., Simoneit, B.R.T. (Eds.), The Gulf and Peninsular Province of the Californias, vol. 47. American Association of Petroleum Geologists, Tulsa, pp. 617–635.

Behrenfeld, M., Falkowski, P., 1997. Photosynthetic rates derived from satellite-based chlorophyll concentration. Limnology and Oceanography 42, 1–20.

Benitez-Nelson, C., Buesseler, K., Karl, D., Andrews, J., 2001. A time-series study of particulate matter export in the North Pacific Subtropical Gyre based on ^{234}Th:^{238}U disequilibrium. Deep Sea Research Part I: Oceanographic Research Papers 48, 2595–2611.

Brandes, J.A., Devol, A.H., 2002. A global marine fixed nitrogen isotopic budget: implications for Holocene nitrogen cycling. Global Biogeochemical Cycles, 16. http://dx.doi.org/10.1029/2001GB001856.

Brandes, J.A., Devol, A.H., Yoshinari, T., Jayakumar, D.A., Naqvi, S.W., 1998. Isotopic composition of nitrate in the central Arabian Sea and eastern tropical North Pacific: a tracer for mixing and nitrogen cycles. Limnology and Oceanography 43, 1680–1689.

Brandhorst, W., 1958. Nitrite accumulation in the northeast tropical Pacific. Nature 182, 679.

Brinton, E., Fleminger, A., Siegel-Causey, D., 1986. The temperate and tropical planktonic biotas of the Gulf of California. CalCOFI Report 27, 228–266.

Buesseler, K., 1991. Do upper-ocean sediment traps provide an accurate record of particle flux? Nature 353, 420–423.
Buesseler, K., 1998. The decoupling of production and particulate export in the surface ocean. Global Biogeochemical Cycles 12, 297–310.
Buesseler, K., Ball, L., Andrews, J., Cochran, J., Hirschberg, D., Bacon, M., Fleer, A., Brzezinski, M., 2001. Upper ocean export of particulate organic carbon and biogenic silica in the Southern Ocean along 170 W. Deep Sea Research Part II: Topical Studies in Oceanography 48, 4275–4297.
Buesseler, K., Antia, A., Chen, M., Fowler, S., Gardner, W., Gustafsson, O., Harada, K., Michaels, A., van der Loeff, R., Sarin, M., 2007a. An assessment of the use of sediment traps for estimating upper ocean particle fluxes. Journal of Marine Research 65, 345–416.
Buesseler, K.O., Antia, A.N., Chen, M., Fowler, S.W., Gardner, W.D., Gustafsson, O., Harada, K., Michaels, A.F., van der Loeff, R., Michiel, S., Manmohan, S., Steinberg, D.K., Trull, T., 2007b. Estimating upper ocean particle fluxes using sediment traps. Journal of Marine Research 65, 345–416.
Capone, D.G., Zehr, J.P., Paerl, H.W., Bergman, B., Carpenter, E.J., 1997. *Trichodesmium*, a globally significant marine cyanobacterium. Science 276, 1221–1229.
Capone, D.G., Subramaniam, A., Montoya, J.P., Voss, M., Humborg, C., Johansen, A.M., Siefert, R.L., Carpenter, E.J., 1998. An extensive bloom of the N_2-fixing cyanobacterium *Trichodesmium erythraeum* in the central Arabian Sea. Marine Ecology Progress Series 172, 281–292.
Carpenter, E.J., Harvey, H.R., Fry, B., Capone, D.G., 1997. Biogeochemical tracers of the marine cyanobacterium *Trichodesmium*. Deep Sea Research I 44, 27–38.
Carpenter, E.J., Subramaniam, A., Capone, D.G., 2004. Biomass and primary productivity of the cyanobacterium, *Trichodesmium* spp., in the southwest tropical N. Atlantic. Deep Sea Research I 51, 173–203.
Casciotti, K., Trull, T., Glover, D., Davies, D., 2008. Constraints on nitrogen cycling at the subtropical North Pacific Station ALOHA from isotopic measurements of nitrate and particulate nitrogen. Deep Sea Research Part II: Topical Studies in Oceanography 55, 1661–1672.
Castro, C., Chavez, F., Collins, C., 2001. Role of the California Undercurrent in the export of denitrified waters from the eastern tropical North Pacific. Global Biogeochemical Cycles 15, 819–830.
Checkley Jr., D.M., Miller, C.A., 1989. Nitrogen isotope fractionation by oceanic zooplankton. Deep Sea Research Part A. Oceanographic Research Papers 36, 1449–1456.
Church, M., Short, C., Jenkins, B., Karl, D., Zehr, J., 2005a. Temporal patterns of nitrogenase gene (nifH) expression in the oligotrophic North Pacific Ocean. Applied and Environmental Microbiology 71, 5362.
Church, M.J., Jenkins, B.D., Karl, D.M., Zehr, J.P., 2005b. Vertical distributions of nitrogen-fixing phylotypes at Stn ALOHA in the oligotrophic North Pacific Ocean. Aquatic Microbial Ecology 38, 3–14.
Church, M., Mahaffey, C., Letelier, R., Lukas, R., Zehr, J., Karl, D., 2009. Physical forcing of nitrogen fixation and diazotroph community structure in the North Pacific subtropical gyre. Global Biogeochemical Cycles, 23. http://dx.doi.org/10.1029/2008GB003418.
Cline, J.D., Richards, F.A., 1972. Oxygen deficient conditions and nitrate reduction in the eastern tropical North Pacific Ocean. Limnology and Oceanography 17, 885–900.
Coale, K.H., Bruland, K.W., 1987. Oceanic stratified euphotic zone as elucidated by ^{234}Th:^{238}U disequilibria. Limnology and Oceanography 32, 189–200.
Codispoti, L.A., 1989. Phosphorus versus nitrogen limitation of new and export production. In: Berger, W.H., Smetacek, V., Wefer, G. (Eds.), Productivity of the Ocean: Past and Present. John Wiley & Sons, Berlin, pp. 377–394.
Codispoti, L.A., 2006. An oceanic fixed nitrogen sink exceeding 400 Tg N a^{-1} vs the concept of homeostasis in the fixed-nitrogen inventory. Biogeosciences Discussions 3, 1203–1246.
Codispoti, L.A., Richards, F.A., 1976. An analysis of the horizontal regime of denitrification in the eastern tropical North Pacific. Limnology and Oceanography 21, 379–388.
Codispoti, L.A., Brandes, J.A., Christensen, J.P., Devol, A.H., Naqvi, S.W.A., Paerl, H.W., Yoshinari, T., 2001. The oceanic fixed nitrogen and nitrous oxide budgets: moving targets as we enter the anthropocene. Scientia Marina 65, 85–105.
Cohen, Y., Gordon, L.I., 1978. Nitrous oxide in the oxygen minimum of the eastern tropical North Pacific: evidence for its consumption during denitrification and possible mechanisms for its production. Deep-Sea Research I 25, 509–524.
DeMaster, D.J., 1991. Measuring biogenic silica in marine sediments and suspended matter. In: Hurd, D.C., Spenser, D.W. (Eds.), Marine Particles: Analysis and Characterization. American Geophysical Union, pp. 363–368.
Deutsch, C., Weber, T., 2012. Nutrient ratios as a tracer and driver of ocean biogeochemistry. Annual Review of Marine Science 4, 113–141.
Deutsch, C., Gruber, N., Key, R.M., Sarmiento, J.L., Ganachaud, A., 2001. Denitrification and N_2 fixation in the Pacific Ocean. Global Biogeochemical Cycles 15, 483–506.
Deutsch, C., Sigman, D.M., Thunell, R., Meckler, A.N., Haug, G.H., 2004. Isotopic constaints on the glacial/interglacial oceanic nitrogen budget. Global Biogeochemical Cycles, 18. http://dx.doi.org/10.1029/2003GB002189.
Deutsch, C., Sarmiento, J., Sigman, D., Gruber, N., Dunne, J., 2007. Spatial coupling of nitrogen inputs and losses in the ocean. Nature 445, 163–167.
Dore, J.E., Brum, J.R., Tupas, L.M., Karl, D.M., 2002. Seasonal and interannual variability in sources of nitrogen supporting export in the oligotrophic subtropical North Pacific Ocean. Limnology and Oceanography 47, 1595–1607.
Duce, R., LaRoche, J., Altieri, K., Arrigo, K., Baker, A., Capone, D., Cornell, S., Dentener, F., Galloway, J., Ganeshram, R., 2008. Impacts of atmospheric anthropogenic nitrogen on the open ocean. Science 320, 893–897.
Dugdale, R., Goering, J., Ryther, J., 1964. High nitrogen fixation rates in the Sargasso Sea and the Arabian Sea. Limnology and Oceanography 9, 507–510.
Duteil, O., Oschlies, A., 2011. Sensitivity of simulated extent and future evolution of marine suboxia to mixing intensity. Geophysical Research Letters 38, L06607.
Eppley, R.W., Peterson, B.J., 1979. Particulate organic matter flux and planktonic new production in the deep ocean. Nature 282, 677–680.
Fernandez, C., Farías, L., Ulloa, O., 2011. Nitrogen fixation in denitrified marine waters. PLoS ONE 6, e20539.
Foster, R., O'Mullen, G., 2008. Nitrogen-fixing and nitrifying symbioses in the marine environment. In: Capone, D., Bronk, D., Mulholland, M., Carpenter, E. (Eds.), Nitrogen in the Marine Environment. Academic Press/Elsevier, San Diego.
Foster, R., Subramaniam, A., Mahaffey, C., Carpenter, E., Capone, D., Zehr, J., 2007. Influence of the Amazon River plume on distributions of free-living and symbiotic cyanobacteria in the western tropical north Atlantic Ocean. Limnology and Oceanography 52, 517–532.
Foster, R., Subramaniam, A., Zehr, J., 2009. Distribution and activity of diazotrophs in the Eastern Equatorial Atlantic. Environmental Microbiology 11, 741–750.
Galloway, J.N., Dentener, F.J., Capone, D.G., Boyer, E.W., Howarth, R.W., Seitzinger, S.P., Asner, G.P., Cleveland, C.C., Green, P.A., Holland, E.A., Karl, D.M., Michaels, A.F., Porter, J.H., Townsend, A.R., Vöosmarty, C.J., 2004. Nitrogen cycles: past, present, and future. Biogeochemistry 70, 153–226.
Ganeshram, R., Pedersen, T., Calvert, S., Murray, J., 1995. Large changes in oceanic nutrient inventories from glacial to interglacial periods. Nature 376, 755–758.
Geider, R.J., Roche, J.L., 2002. Redfield revisited: variability of C:N:P in marine microalgae and its biochemical basis. European Journal of Phycology 37, 1–17.
Gnanadesikan, A., Dunne, J., John, J., 2012. Understanding why the volume of suboxic waters does not increase over centuries of global warming in an Earth System Model. Biogeosciences 9, 1159–1172.
Gruber, N., 2004. The dynamics of the marine nitrogen cycle and its influence on atmospheric CO_2 variations. The Ocean Carbon Cycle and Climate, 97–148.
Gruber, N., Sarmiento, J.L., 1997. Global patterns of marine nitrogen fixation and denitrification. Global Biogeochemical Cycles 11, 235–266.
Halsey, K.H., Milligan, A.J., Behrenfeld, M.J., 2010. Physiological optimization underlies growth rate-independent chlorophyll-specific gross and net primary production. Photosynthesis Research 103, 125–137.
Hamersley, M.R., Turk, K., Leinweber, A., Gruber, N., Zehr, J., Gunderson, T., Capone, D., 2011. Nitrogen fixation within the water column associated with two hypoxic basins in the Southern California Bight. Aquatic Microbial Ecology 63, 193–205.
Jayakumar, A., Al-Rshaidat, M., Ward, B.B., Mulholland, M.R., 2012. Diversity, distribution and expression of diazotroph nifH genes in oxygen deficient waters of the Arabian Sea. FEMS Microbiology Ecology, doi: 10.1111.
Kara, A.B., Rochford, P.A., Hurlburt, H.E., 2000. An optimal definition for ocean mixed layer depth. Journal of Geophysical Research 105, 16803–16821.
Karl, D., Letelier, R., 2008. Nitrogen fixation-enhanced carbon sequestration in low nitrate, low chlorophyll seascapes. Marine Ecology Progress Series 364, 257–268.
Kienast, M., 2000. Unchanged nitrogen isotopic composition of organic matter in the South China Sea during the last climatic cycle: global implications. Paleoceanography 15, 244–253.
Krauk, J.M., Villareal, T.A., Sohm, J.A., Montoya, J.P., Capone, D.G., 2006. Plasticity of N:P ratios of laboratory and field populations of *Trichodesmium* spp. Aquatic Microbial Ecology 42, 243–253.
Krishnamurthy, A., Moore, J.K., Zender, C.S., Luo, C., 2007. Effects of atmospheric inorganic nitrogen deposition on ocean biogeochemistry. Journal of Geophysical Research 112, G02019.
Liu, H.-S., 1992. Frequency variations of the Earth's obliquity and the 100-kyr ice-age cycles. Nature 358, 397–399.
Lomas, M., Moran, S., 2011. Evidence for aggregation and export of cyanobacteria and nano-eukaryotes from the Sargasso Sea euphotic zone. Biogeosciences 8, 203–216.
Luo, Y.-W., Doney, S.C., Anderson, L.A., Benavides, M., Bode, A., Bonnet, S., Bostrom, K.H., Bottjer, D., Capone, D.G., Carpenter, E.J., Chen, Y.L., Church, M.J., Dore, J.E., Falcon, L.I., Fernandez, A., Foster, R.A., Furuya, K., Gomez, F., Gundersen, K., Hynes, A.M., Karl, D.M., Kitajima, S., Langlois, R.J., LaRoche, J., Letelier, R.M., Maranon, E., McGillicuddy Jr., D.J., Moisander, P.H., Moore, C.M., Mourino-Carballido, B., Mulholland, M.R., Needoba, J.A., Orcutt, K.M., Poulton, A.J., Raimbault, P., Rees, A.P., Riemann, L., Shiozaki, T., Subramaniam, A., Tyrrell, T., Turk-Kubo, K.A., Varela, M., Villareal, T.A., Webb, E.A., White, A.E., Wu, J., Zehr, J.P., 2012. Database of diazotrophs in global ocean: abundances, biomass and nitrogen fixation rates. Earth System Science Data Discussions 5, doi:10.5194.
Lyons, G., Benitez-Nelson, C., Thunell, R., 2011. Phosphorus composition of sinking particles in the Guaymas Basin, Gulf of California. Limnology and Oceanography 56, 1093–1105.
Malinverno, E., Prahl, F.G., Popp, B.N., Ziveri, P., 2008. Alkenone abundance and its relationship to the coccolithophore assemblage in Gulf of California surface waters. Deep-Sea Research I 55, 1118–1130.
Marra, J., 2002. Approaches to the measurement of plankton production. In: Williams, P.J.L., Thomas, D.N., Reynolds, C.S. (Eds.), Phytoplankton Productivity: Carbon Assimilation in Marine and Freshwater Ecosystems. Blackwell, Oxford, pp. 78–108.
Mee, L.D., Cortes-Altamirano, R., Garcia de la Parra, L.M., 1984. Dinitrogen fixation in a eutrophic tropical bay. Estuarine, Coastal and Shelf Science 19, 477–483.

Please cite this article in press as: White, A.E., et al. Nitrogen fixation in the Gulf of California and the Eastern Tropical North Pacific. Prog. Oceanogr. (2012), http://dx.doi.org/10.1016/j.pocean.2012.09.002

Middelburg, J., Soetaert, K., Herman, P., Heip, C., 1996. Denitrification in marine sediments: a model study. Global Biogeochemical Cycles 10, 661–673.

Minagawa, M., Wada, E., 1986. Nitrogen isotope ratios of red tide organisms in the East China Sea: a characterization of biological nitrogen fixation. Marine Chemistry 19, 245–259.

Mohr, W., Großkopf, T., Wallace, D.W.R., LaRoche, J., 2010. Methodological underestimation of oceanic nitrogen fixation rates. PLoS ONE 5, e12583.

Moisander, P.H., Beinart, R.A., Hewson, I., White, A.E., Johnson, K.S., Carlson, C.A., Montoya, J.P., Zehr, J.P., 2010. Unicellular cyanobacterial distributions broaden the oceanic N_2 fixation domain. Science 327, 1512–1514.

Montoya, J.P., Voss, M., Kahler, P., Capone, D.G., 1996. A simple, high-precision, high sensitivity tracer assay for N_2 fixation. Applied and Environmental Microbiology 62, 986–993.

Moore, J., Doney, S., 2007. Iron availability limits the ocean nitrogen inventory stabilizing feedbacks between marine denitrification and nitrogen fixation. Global Biogeochemical Cycles, 21. http://dx.doi.org/10.1029/2006GB002762.

Mulholland, M., 2007. The fate of nitrogen fixed by diazotrophs in the ocean. Biogeosciences 4, 37–51.

Needoba, J., Foster, R., Sakamoto, C., Zehr, J., Johnson, K., 2007. Nitrogen fixation by unicellular diazotrophic cyanobacteria in the temperate oligotrophic North Pacific Ocean. Limnology and Oceanography 52, 1317–1327.

Paulmier, A., Ruiz-Pino, D., 2009. Oxygen minimum zones (OMZs) in the modern ocean. Progress in Oceanography 80, 113–128.

Pike, S.M., Buesseler, K.O., Andrews, J.A., Savoye, N., 2005. Quantification of ^{234}Th recovery in small volume sea water samples by inductively coupled plasma mass spectrometry. Journal of Radioanalytical and Nuclear Chemistry 263, 355–360.

Popp, B.N., Westley, M.B., Toyoda, S., Miwa, T., Dore, J.E., Yoshida, N., Rust, T.M., Sansone, F.J., Russ, M.E., Ostrom, N.E., 2002. Nitrogen and oxygen isotopomeric constraints on the origins and sea-to-air flux of N_2O in the oligotrophic subtropical North Pacific gyre. Global Biogeochemical Cycles 16, 1064.

Prahl, F.G., Dymond, J., Sparrow, M.A., 2000. Annual biomarker record for export production in the central Arabian Sea. Deep Sea Research Part II: Topical Studies in Oceanography 47, 1581–1604.

Prahl, F.C., Popp, B.N., Karl, D.M., Sparrow, M.A., 2005. Ecology and biogeochemistry of alkenone production at Station ALOHA. Deep Sea Research I 52, 699–719.

Redfield, A.C., 1958. The biological control of chemical factors in the environment. American Scientist 46, 205–221.

Richardson, T.L., Jackson, G.A., 2007. Small phytoplankton and carbon export from the surface ocean. Science 315, 838.

Roden, G.I., 1958. Oceanographic and meteorological aspects of the Gulf of California. Journal of Marine Research 18, 10–35.

Savoye, N., Benitez-Nelson, C., Burd, A., Cochran, J., Charette, M., Buesseler, K., Jackson, G., Roy-Barman, M., Schmidt, S., Elskens, M., 2006. Th-234 sorption and export models in the water column: a review. Marine Chemistry 100, 234–249.

Scharek, R., Tupas, L., Karl, D.M., 1999. Diatom fluxes to the deep sea in the oligotrophic North Pacific gyre at Station ALOHA. Marine Ecology Progress Series 182, 55–67.

Shi, T., Ilikchyan, I., Rabouille, S., Zehr, J., 2010. Genome-wide analysis of diel gene expression in the unicellular N_2-fixing cyanobacterium *Crocosphaera watsonii* WH 8501. The ISME Journal 4, 621–632.

Sigman, D., Casciotti, K., Andreani, M., Barford, C., Galanter, M., Böhlke, J., 2001. A bacterial method for the nitrogen isotopic analysis of nitrate in seawater and freshwater. Analytical Chemistry 73, 4145–4153.

Sigman, D.M., Granger, J., DiFiore, P.J., Lehmann, M.M., Ho, R., Cane, G., Van Geen, A., 2005. Coupled nitrogen and oxygen isotope measurements of nitrate along the eastern North Pacific margin. Global Biogeochemical Cycles 19, GB4022, doi: 4010.1029/2005GB2458.

Small, L.F., Knauer, G.A., Tuel, M.D., 1987. The role of sinking fecal pellets in stratified euphotic zones. Deep-Sea Research I 34, 1705–1712.

Strickland, J.D.H., Parsons, T.R., 1972. A Practical Handbook of Seawater Analysis. Fisheries Research Board of Canada, Ottawa.

Struck, U., Pollehne, F., Bauerfeind, E., 2004. Sources of nitrogen for the vertical particle flux in the Gotland Sea (Baltic Proper) – results from sediment trap studies. Journal of Marine Systems 45, 91–101.

Thomas, W.H., 1966. Denitrification in the northeastern tropical Pacific Ocean. Deep-Sea Research and Oceanographic Abstracts 13, 1109–1114.

Thunell, R.C., 1998. Seasonal and annual variability in particle fluxes in the Gulf of California: a response to climate forcing. Deep-Sea Research I 45, 2059–2083.

Turley, C., Mackie, P., 1995. Bacterial and cyanobacterial flux to the deep NE Atlantic on sedimenting particles. Deep Sea Research Part I: Oceanographic Research Papers 42, 1453–1474.

Tyrrell, T., 1999. The relative influences of nitrogen and phosphorus on oceanic primary production. Nature 400, 525–531.

Uitz, J., Huot, Y., Bruyant, F., Babin, M., Claustre, H., 2008. Relating phytoplankton photophysiological properties to community structure on large scales. Limnology and Oceanography 53, 614–630.

Van Mooy, B.A.S., Keil, R.G., Devol, A.H., 2002. Impact of suboxia on sinking particulate organic carbon: enhanced carbon flux and preferential degradation of amino acids via denitrification. Geochimica et Cosmochimica Acta 66, 457–465.

Wada, E., Hattori, A., 1976. Natural abundance of ^{15}N in particulate organic matter in the North Pacific Ocean. Geochimica et Cosmochimica Acta 40, 249–251.

Waples, J., Benitez-Nelson, C.R., Savoye, N., Rutgers van der Loeff, M., Baskaran, M., Gustafsson, Ö., 2006. An introduction to the application and future use of ^{234}Th in aquatic systems. Marine Chemistry 100, 166–189.

Weber, T.S., Deutsch, C., 2010. Ocean nutrient ratios governed by plankton biogeography. Nature 467, 550–554.

Westberry, T., Siegel, D.A., 2006. Spatial and temporal distribution of *Trichodesmium* blooms in the world's oceans. Global Biogeochemical Cycles, 20. http://dx.doi.org/10.1029/2005GB002673.

White, A.E., Spitz, Y.H., Karl, D.M., Letelier, R.M., 2006. Flexible elemental stoichiometry in *Trichodesmium* spp. and its ecological implications. Limnology and Oceanography 51, 1777–1790.

White, A.E., Spitz, Y.H., Letelier, R.M., 2007. What factors are driving summer phytoplankton blooms in the North Pacific Subtropical Gyre. Journal of Geophysical Research 112, C12006.

White, A.E., Prahl, F.G., Letelier, R.M., Popp, B.N., 2007a. Summer surface waters in the Gulf of California: prime habitat for biological N_2 fixation. Global Biogeochemical Cycles, 21. http://dx.doi.org/10.1029/2006GB002779.

Wright, S.W., Jeffrey, S.W., Mantoura, R.F.C., Llewellyn, C.A., Bjornland, T., Repeta, D., Welschmeyer, N., 1991. Improved HPLC method for the analysis of chlorophylls and carotenoids from marine phytoplankton. Marine Ecology Progress Series 77, 183–196.

Zehr, J.P., Mellon, M.T., Zani, S., 1998. New nitrogen-fixing microorganisms detected in oligotrophic oceans by amplification of nitrogenase (nifH) genes. Applied and Environmental Microbiology 64, 3444–3450.

Please cite this article in press as: White, A.E., et al. Nitrogen fixation in the Gulf of California and the Eastern Tropical North Pacific. Prog. Oceanogr. (2012), http://dx.doi.org/10.1016/j.pocean.2012.09.002